

Budget of organic carbon in a polluted atmosphere: Results from the New England Air Quality Study in 2002

J. A. de Gouw,^{1,2} A. M. Middlebrook,¹ C. Warneke,^{1,2} P. D. Goldan,¹ W. C. Kuster,¹ J. M. Roberts,¹ F. C. Fehsenfeld,¹ D. R. Worsnop,³ M. R. Canagaratna,³ A. A. P. Pszenny,^{4,5} W. C. Keene,⁶ M. Marchewka,⁷ S. B. Bertman,⁷ and T. S. Bates⁸

Received 22 November 2004; revised 28 March 2005; accepted 14 June 2005; published 30 August 2005.

[1] An extensive set of volatile organic compounds (VOCs) and particulate organic matter (POM) was measured in polluted air during the New England Air Quality Study in 2002. Using VOC ratios, the photochemical age of the sampled air masses was estimated. This approach was validated (1) by comparing the observed rates at which VOCs were removed from the atmosphere with the rates expected from OH oxidation, (2) by comparing the VOC emission ratios inferred from the data with the average composition of urban air, and (3) by the ability to describe the increase of an alkyl nitrate with time in terms of the chemical kinetics. A large part of the variability observed for oxygenated VOCs (OVOCs) and POM could be explained by a description that includes the removal of the primary anthropogenic emissions, the formation and removal of secondary anthropogenic species, and a biogenic contribution parameterized by the emissions of isoprene. The OVOC sources determined from the data are compared with the available literature, and a satisfactory agreement is obtained. The observed sub- μm POM was highly correlated with secondary anthropogenic gas-phase species, strongly suggesting that the POM was from secondary anthropogenic sources. The results are used to describe the speciation and total mass of gas- and particle-phase organic carbon as a function of the photochemical age of an urban air mass. Shortly after emission the organic carbon mass is dominated by primary VOCs, while after two days the dominant contribution is from OVOCs and sub- μm POM. The total measured organic carbon mass decreased by about 40% over the course of two days. The increase in sub- μm POM could not be explained by the removal of aromatic precursors alone, suggesting that other species must have contributed and/or that the mechanism for POM formation is more efficient than previously assumed.

Citation: de Gouw, J. A., et al. (2005), Budget of organic carbon in a polluted atmosphere: Results from the New England Air Quality Study in 2002, *J. Geophys. Res.*, *110*, D16305, doi:10.1029/2004JD005623.

1. Introduction

[2] Volatile organic compounds (VOCs) in the Earth's atmosphere are emitted from a wide variety of man-made and natural sources. The atmospheric lifetimes of VOCs

vary from minutes to years, and are limited by chemical reactions, photolysis, and deposition. Secondary organic species, including oxygenated VOCs (OVOCs), organic nitrates and particulate organic matter (POM), are formed from the photo-oxidation of many VOCs. In polluted atmospheres the cycle of gas- and particle-phase organic carbon is closely coupled with the formation of ozone and aerosol, which are significant air pollutants and are also important factors in the Earth's climate system. (The term organic carbon refers in this paper to the combined carbon in the gas and particle phase.) Additionally, the photochemistry of organic carbon influences the oxidizing capacity of the background atmosphere, which limits the lifetime of greenhouse gases such as methane. Consequently, it is essential to understand the budget of organic carbon quantitatively, but to date our knowledge is rather limited. The primary emissions of VOCs from anthropogenic [Harley *et al.*, 1992; Kristensson *et al.*, 2004] and biogenic sources [Guenther *et al.*, 1995; Fall, 1999] are reasonably well known, and the rates at which these species are removed are

¹Aeronomy Laboratory, NOAA, Boulder, Colorado, USA.

²Also at Cooperative Institute for Research in Environmental Sciences, University of Colorado, Boulder, Colorado, USA.

³Aerodyne Research Inc., Billerica, Massachusetts, USA.

⁴Institute for the Study of Earth, Oceans, and Space, University of New Hampshire, Durham, New Hampshire, USA.

⁵Also at Mount Washington Observatory, North Conway, New Hampshire, USA.

⁶Department of Environmental Sciences, University of Virginia, Charlottesville, Virginia, USA.

⁷Department of Chemistry, Western Michigan University, Kalamazoo, Michigan, USA.

⁸Pacific Marine Environmental Laboratory, NOAA, Seattle, Washington, USA.

quantitatively understood [Atkinson, 2000, and references therein]. The formation of secondary species has been more difficult to understand, partly because the techniques to reliably measure OVOCs and particulate organic matter (POM) have only been developed in recent years. There is presently very limited insight into the ultimate fate of organic carbon: deposition, continued chemical reactions leading to the formation of CO and CO₂, and/or uptake by aerosol followed by deposition. The suspicion is that aerosol uptake and deposition account for a large sink of gas-phase VOCs, partly because second- and third-generation gas-phase oxidation products have not been observed in the abundances expected from the precursor concentrations. Reliable measurements of difunctional VOCs are very difficult, however, and it is possible that part of the organic carbon transforms into a gas-phase component of air that cannot be detected with present techniques. It is clearly important to determine the ultimate fate of organic carbon: if the organic carbon remains as a reactive intermediate in the gas phase, the production of ozone and other products would be expected to continue. Alternatively, if converted to relatively inert carboxylic acids and/or incorporated into aerosols, it can be lost via deposition to the surface or react further in the condensed phase with entirely different atmospheric implications [Faust et al., 1993; Ravishankara, 1997].

[3] During the New England Air Quality Study (NEAQS) in 2002 a suite of organic species was measured onboard the NOAA research ship *Ronald H. Brown* along the northeastern U.S. coast. The measured gas-phase species included nonmethane hydrocarbons, oxygenated VOCs, carboxylic acids, alkyl nitrates and several peroxyacyl nitrate (PAN) compounds. Many species were measured by more than one instrument and these measurements were carefully compared [de Gouw et al., 2003a]. Particulate organic matter (POM) was measured on-line by aerosol mass spectrometry (AMS); and particulate organic carbon (POC) by filter sampling and subsequent laboratory analysis. On average, POC accounted for about half of the sub- μm aerosol mass at 55% relative humidity [Quinn and Bates, 2003], and thus it is clearly important to understand the sources quantitatively.

[4] In this work a combined analysis of organic carbon in the gas and particle phase is developed. Using (1) the measurements of an inert pollution tracer (acetylene), (2) hydrocarbon ratios to estimate the photochemical age [Roberts et al., 1984], and (3) the chemical kinetics of the reactions involved, both the removal of primary anthropogenic VOCs and the production of secondary anthropogenic VOCs are described. The analysis of the OVOC and POM measurements is complicated by the potentially significant biogenic sources of these species. Assuming that the biogenic sources are proportional to the emissions of isoprene, the biogenic fraction of the measured OVOC and POM concentrations are separately determined. The approach is verified by analyzing PAN compounds, which have known anthropogenic and biogenic precursors [Williams et al., 1997]. The anthropogenic and biogenic emission ratios for OVOCs derived from the NEAQS data are compared with emission ratios reported in the literature. One of the results of the analysis

is a description of the evolution of the total and speciated organic carbon in an air mass as it is processed. The increase in the mass associated with POM is compared with the formation yields for different precursors that have been reported in the literature [Odum et al., 1997; Seinfeld and Pandis, 1998].

[5] The NEAQS data set is uniquely suited to be analyzed in this manner because of the large number of organic species that were measured onboard the *Ronald H. Brown*, and because of the ship-based sampling of continental air, which allowed air masses with varying degrees of photochemical processing to be characterized without additional continental emissions in between the major sources and the sampling location. In addition, precipitation, which removes particles more efficiently than most VOCs, was infrequent during NEAQS. Potentially complicating factors in the analysis, which will be briefly addressed, include the complex meso-scale meteorology of the New England coastal region [Angevine et al., 2004], the presence of oceanic VOC emissions [Bonsang et al., 1988; Zhou and Mopper, 1997], and the potential for halogen chemistry involving sea salt [Sander et al., 2003].

2. Methods

2.1. Ship-Based Measurements

[6] The cruise track of the NOAA research vessel *Ronald H. Brown* during NEAQS, and the measurements used in the paper have been described in detail elsewhere [de Gouw et al., 2003a; Warneke et al., 2004; Goldan et al., 2004], and only the details pertinent to the current work are presented here. The cruise track of the NOAA ship *Ronald H. Brown* consisted of two legs: Charleston, SC – Portsmouth, NH between July 12 and 26 of 2002, and Portsmouth - Charleston from July 29 until August 10. Most of this time was spent along the coast of New Hampshire and Massachusetts (July 17–August 6) and on a single transect along the coast of Maine (July 24–25). The sampled air masses had been impacted by major urban areas such as New York City and Boston, and by biogenic emissions in New Hampshire and Maine [Warneke et al., 2004; Goldan et al., 2004]. Power plants and ocean vessels were found to be very minor sources of VOCs.

[7] Nonmethane hydrocarbons and oxygenated species were measured by on-line gas chromatography-mass spectrometry (GC-MS) using a new, automated instrument that was deployed for the first time during NEAQS. A detailed description of the set-up and an overview of the measurement results obtained during NEAQS have been presented elsewhere [Goldan et al., 2004]. Briefly, organic species were collected cryogenically for subsequent capillary chromatographic analysis by two parallel sampling systems. The first channel used a flame-ionization detector (FID) for the analysis of C₂-C₅ alkanes, C₂-C₄ alkenes and acetylene. The second channel used an Agilent 5973 quadrupole mass spectrometer for the detection of heavier alkanes and alkenes up to C₁₀, C₁-C₇ alkyl nitrates, C₆-C₉ aromatics, light alcohols, aldehydes, ketones, dimethyl sulfide and acetonitrile. Samples were collected and immediately analyzed each half hour. The system was calibrated using

numerous gas standards; the measurement precision was typically 2% and the overall accuracy 10%. The detection limit of the system was below 1 pptv (parts per trillion by volume) for most compounds detected.

[8] Formic and acetic acids together with a suite of other soluble reactive trace gases (HNO_3 , NH_3 , HCl) were sampled over 2-hour intervals with tandem mist chambers containing deionized water and analyzed on board the ship by high-performance ion chromatography (MC-IC [Keene *et al.*, 2004]). Gas-phase mixing ratios were calculated based on the corresponding volumes of air sampled. Performance characteristics of standard mist chamber samplers for carboxylic acids have been critically evaluated [Keene *et al.*, 1989]. Collection efficiencies were greater than 95%, precision averaged about $\pm 15\%$, and detection limits averaged about 12 pptv.

[9] Williams *et al.* [2000] and Roberts *et al.* [2002] have described the methods for the measurement of the peroxyacyl nitrates. In summary the instrument uses capillary gas chromatographic separation, followed by electron capture detection (GC-ECD). The sample loop in the instrument was continuously flushed at 1 STP L min^{-1} , and the content was injected into the GC column every 10 minutes. The instrument response to peroxyacetyl nitrate (PAN) was calibrated routinely using a modified acetone/CO/NO photolysis source which is based on the calibrated NO mixing ratio and known conversion efficiency ($93 \pm 3\%$) [Roberts *et al.*, 2002]. The calibrations of PPN (peroxy propionyl nitrate), PiBN (peroxy isobutyryl nitrate) and MPAN (peroxy methacryloyl nitrate) were based on relative response factors that had been determined in the laboratory, and have been consistent within 5% over several different field campaigns. Detection limits for PAN, PPN, PiBN and MPAN were 4 pptv and the overall uncertainties were $\pm(4 \text{ pptv} + 15\%)$ for PAN, and $\pm(4 \text{ pptv} + 20\%)$ for PPN, PiBN and MPAN.

[10] A subset of organic species was measured at a higher frequency with a proton-transfer-reaction mass spectrometry (PTR-MS) instrument. These measurements were compared with the results from the respective alternative methods, and most of the measurements compared well [de Gouw *et al.*, 2003a]. The reader is referred to this work for a detailed description of the PTR-MS measurements. The PTR-MS data for acetaldehyde were a factor of 1.56 higher than the GC-MS acetaldehyde data due to a calibration inaccuracy. The GC-MS calibration was based on more than one calibration gas mixture and was therefore deemed more reliable. The GC-MS data for acetaldehyde in ambient air contained several large peaks during a relatively clean period that were not observed by the PTR-MS [de Gouw *et al.*, 2003a]. For these reasons the PTR-MS data are used in the present study, but the calibration has been adjusted for better overall agreement with the GC-MS data.

[11] Several different combinations of impactors, filters and a denuder were used to sample sub- and super- μm particulate organic carbon (POC) and elemental carbon on the ship. The impactor sampling periods averaged 7.7 h and varied between 3 and 20 hours. For the POC data sub- μm refers to particles with an aerodynamic diameter, D_{aero} of less than $1.1 \mu\text{m}$ at 55% relative humidity (RH), and super- μm refers to particles with $1.1 \mu\text{m} < D_{\text{aero}} < 10 \mu\text{m}$ at

55% RH. The samples were analyzed onboard the *Ronald H. Brown* using a Sunset Labs thermal/optical analyzer. A detailed description of the sampling and analysis set-up has been given elsewhere [Bates *et al.*, 2002; Schauer *et al.*, 2003]. More than 80% of POC, measured from the impactor samples during NEAQS, was associated with sub- μm particles.

[12] Measurements of the nonrefractory components of the sub- μm aerosol (organics, nitrate, sulfate and ammonium) were performed by aerosol mass spectrometry (AMS) [Jayne *et al.*, 2000; Jimenez *et al.*, 2003] with one data point recorded every two minutes. An overview of the measurements will be presented elsewhere, and only a brief discussion of the measurement results related to the sub- μm particulate organic matter (POM) is presented here. The AMS data for sulfate and ammonium were highly correlated ($r = 0.96$ and 0.95 , respectively) with the online particle-into-liquid sampler (PILS) ion chromatography measurements. For the NEAQS2002 field study the AMS collection efficiencies, defined as the fraction of particles entering the instrument that is detected, were obtained from the slopes of linear regressions of the AMS versus PILS data for sulfate and ammonium. The AMS/PILS slopes for both species were close to 0.8 for the first leg of the study and close to 1 for the second leg of the study. Based on examining size-resolved aerosol composition data from an impactor, a likely explanation of the difference in collection efficiencies for the two legs is that there was some particle mass between the two size cut-off points of the AMS and PILS instruments ($\sim 0.5 \mu\text{m}$ and $1.1 \mu\text{m}$, respectively) during the first leg but not during the second leg. Since sulfate and ammonium appeared to be internally mixed with the organic material, the same AMS collection efficiencies were applied for POM. There is some uncertainty in the AMS relative ionization efficiency for POM, which is defined as the ionization efficiency for POM (in units of ions molecule $^{-1}$) divided by the ionization efficiency for nitrate. Laboratory studies have shown the AMS relative ionization efficiency to vary from 1.3 for oxidized organic species to 1.9 for hydrocarbons (P. Silva, personal communication). However, most of the POM during NEAQS was oxidized and, hence, an ionization efficiency of 1.4 was used. In agreement with the results from Quinn and Bates [2003], POM was found to be the dominant aerosol component measured by AMS during NEAQS. Although the AMS instrument had a smaller size cut point than the impactor sampler and the relative humidity during sampling was not controlled for the AMS, the sub- μm POM measured by AMS correlated well with the sub- μm POC measured from the impactor samples: the linear correlation coefficient (r) was 0.93. The Sunset Labs instrument measures organic carbon (units $\mu\text{g C m}^{-3}$), whereas the AMS measures organic mass (units $\mu\text{g m}^{-3}$) including the mass of organic carbon, oxygen and hydrogen. The POM/POC ratio was determined to be 1.78 ± 0.13 from a scatterplot of the two parameters, which is in the range of values from previous studies [Turpin and Lim, 2001].

2.2. Data Description

[13] In this work a description of the data is presented that explains a large part of the variability observed for all VOCs

and POM using a limited number of parameters and the measurements of six key gas-phase species (three anthropogenic and three biogenic). As much as possible, the parameters used are taken from or compared with the existing literature on emissions and chemical kinetics. In addition, the description is based on the following assumptions:

[14] 1. Urban and biogenic emissions were the dominant sources of organic carbon in the study region.

[15] 2. The speciation of VOC emissions was the same for all cities in the region. The magnitude of urban emissions was proportional to the emissions of acetylene.

[16] 3. The removal of VOCs was governed by the reaction with OH radicals.

[17] 4. The photochemical age of the sampled air masses can be described by the measured ratio between benzene and toluene.

[18] 5. Biogenic sources of OVOCs and POM were proportional to the emissions of isoprene, i.e. they had the same regional distribution and dependence on sunlight and temperature. Details of the assumptions and their limitations are discussed in the remainder of this section.

[19] Urban and biogenic emissions were found to be the dominant sources of VOCs during NEAQS (assumption 1). Biomass burning had a negligible impact during the study period, evidenced by relatively low mixing ratios of acetonitrile, a proven indicator for biomass burning [de Gouw *et al.*, 2003b]. A large biomass burning event affected New England during early July 2002 [DeBell *et al.*, 2004], but the influence was no longer detected during NEAQS. Point sources, such as power plants and ocean ships, were found to be minor sources of VOCs. Ocean emissions [Bonsang *et al.*, 1988; Zhou and Mopper, 1997], long-range transport and background atmospheric formation [Singh *et al.*, 2001] can all be sources of VOCs: during periods when the sampled air masses did not come from the continent, the measurements of some VOCs were nonzero and relatively constant. These constant backgrounds are incorporated in the description presented here.

[20] Regional differences in the speciation of urban VOC emissions are generally only subtle and are a minor source of uncertainty in the analysis (assumption 2). Evidence for this statement will be shown in this paper, when the VOC emission ratios inferred from the NEAQS data are compared with literature values. Acetylene is used here as an indicator of urban emissions. It is a relatively inert VOC and comes mostly from automobile exhaust, the dominant source of VOCs in a city [Harley *et al.*, 1992]. Other relatively inert VOCs such as ethane and propane are mostly released from waste and natural gas use [Harley *et al.*, 1992], and show more variable emission ratios than most other anthropogenic VOCs.

[21] Warneke *et al.* [2004] have shown that for all anthropogenic VOCs the reaction with OH was the dominant loss mechanism during NEAQS (assumption 3). Reactions with nitrate (NO₃) radicals at night were minor sinks for anthropogenic VOCs, a large fraction of which consists of saturated and aromatic hydrocarbons. However, NO₃ reactions were very significant for VOCs from

biogenic origin, most of which contain (multiple) double bonds. The importance of NO₃ chemistry has some implications for our use of isoprene as an indicator of biogenic emissions, as will be discussed further below in this section.

[22] Using the observed ratio between toluene and benzene (assumption 4), the photochemical age, Δt , of the sampled air masses is estimated in this work by [Roberts *et al.*, 1984]:

$$\Delta t = \frac{1}{[\text{OH}](k_{\text{toluene}} - k_{\text{benzene}})} \times \left[\ln \left(\frac{[\text{toluene}]}{[\text{benzene}]} \right) \Big|_{t=0} - \ln \left(\frac{[\text{toluene}]}{[\text{benzene}]} \right) \right], \quad (1)$$

where [OH] is the average concentration of hydroxyl radicals, and k_{toluene} and k_{benzene} are the rate coefficients for the reaction of OH with toluene ($5.63 \times 10^{-12} \text{ cm}^3 \text{ molecule}^{-1} \text{ s}^{-1}$) and benzene ($1.22 \times 10^{-12} \text{ cm}^3 \text{ molecule}^{-1} \text{ s}^{-1}$), respectively [Atkinson and Arey, 2003]. The emission ratio of toluene to benzene (3.7 ± 0.3) was derived using NEAQS data from several plumes that came directly from urban centers at a time when oxidation processes were at a minimum. This ratio is in good agreement with recent tunnel studies [Kristensson *et al.*, 2004]. The 24-hour averaged concentration of OH was taken as $3 \times 10^6 \text{ molecules cm}^{-3}$ and was estimated from the NEAQS data set [Warneke *et al.*, 2004]. The value of OH determines the photochemical age directly, but many of the results in this paper depend on the relative rather than the absolute values of Δt , as will be shown further below. Several authors have pointed out the limitations of using hydrocarbon ratios to estimate the age of an air mass [McKeen and Liu, 1993; McKeen *et al.*, 1996; Ehhalt *et al.*, 1998]. Notably, the mixing of qualitatively different air masses can have similar effects as chemical reactions on the atmospheric composition. McKeen *et al.* [1996] showed that the characteristic time for dilution with background air is about 2.5 days, which is longer than most of the processes this paper focuses on. Nevertheless, the assumption that the effects of mixing can be ignored should be treated with some caution. Finally, halogen chemistry is assumed to be an insignificant sink for VOCs in this work. The reaction of toluene with Cl radicals is efficient and the rate coefficient is four orders of magnitude higher than that for benzene and Cl [Shi and Bernhard, 1997]. Consequently, Cl radical chemistry can affect the photochemical age based on toluene/benzene ratios, but its effect is expected to be small. For example, at an average Cl concentration of $10^4 \text{ molecules cm}^{-3}$, the inferred photochemical age of an air mass would be overestimated by only about 3%.

[23] At present there are no regional estimates of biogenic OVOC emissions, and our assumption (5) that the emissions are proportional to those of isoprene may be reasonable but is very uncertain. In addition, isoprene is extremely reactive and thus a poorly conserved indicator of biogenic emissions. To correct for this effect we have extrapolated the observed isoprene mixing ratios back to the source (isoprene_{source}) using the measurements of isoprene photo-products, methyl vinyl ketone (MVK) and methacrolein

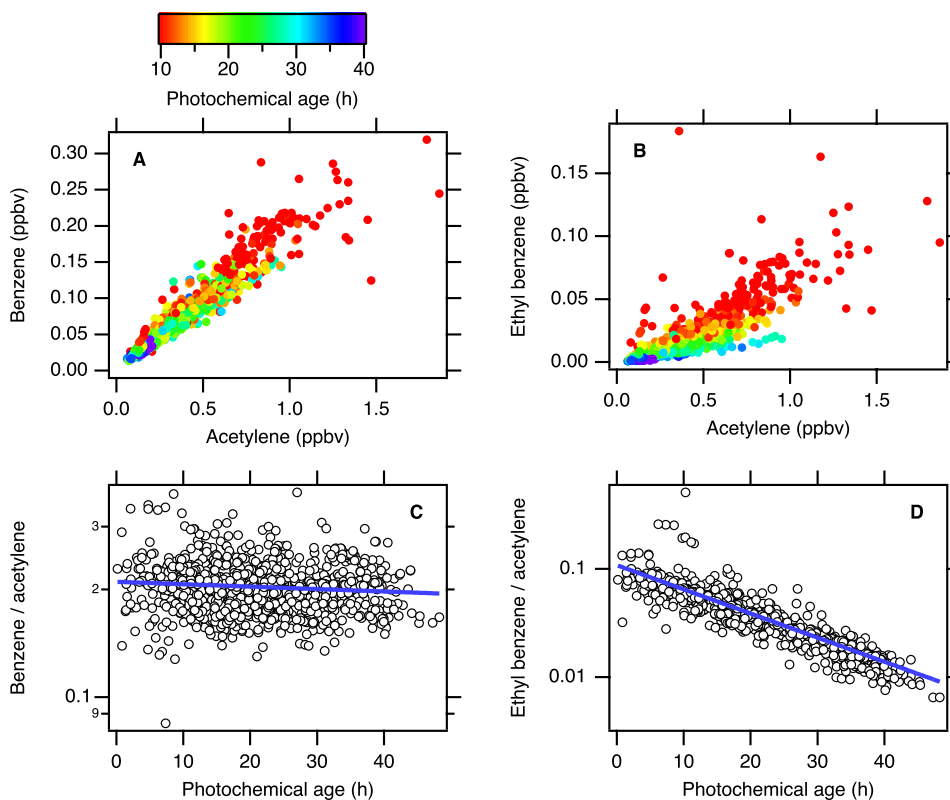
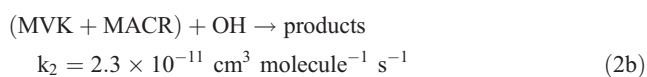
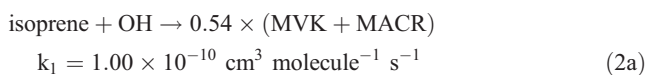


Figure 1. Scatterplots versus acetylene of (a) benzene and (b) ethyl benzene. The data points are color-coded by the photochemical age derived from measured benzene/toluene ratios. (c and d) Benzene/acetylene and ethyl benzene/acetylene ratios versus the photochemical age, along with the results from a fit of equation (3) to the data.

(MACR), and the sequential reaction model described by *Stroud et al.* [2001]:



From the measured ratio between MVK + MACR and isoprene, the time since emission can be determined, and the observed isoprene mixing ratio can be extrapolated back to the source. The calculation only accounts for the chemical conversion by OH radicals of isoprene and its photoproducts, and not for dilution effects. The parameter $\text{isoprene}_{\text{source}}$ is thus likely a lower estimate of the isoprene mixing ratios at the time of emission. However, the OVOCs that are co-emitted with isoprene are subject to the same dilution, and the OVOC/ $\text{isoprene}_{\text{source}}$ ratio should not be affected. A more important limitation of this approach is that equations (2a) and (2b) are only valid during the daytime, whereas *Warneke et al.* [2004] have shown that a significant fraction of isoprene and its photoproducts are removed by NO_3 at night, in which case the kinetics are entirely different from equations (2a) and (2b). It is also important to note that the parameter $\text{isoprene}_{\text{source}}$ is not just

an indicator of primary biogenic emissions: its value is determined by the measured mixing ratios of isoprene, MVK and MACR, with the latter two often having the largest influence. The removal of isoprene in the atmosphere is so rapid that it is impossible to differentiate between primary and secondary OVOC sources using measurements that are typically an hour downwind of the emissions. The parameter $\text{isoprene}_{\text{source}}$ is therefore an indicator of both primary and secondary biogenic sources. In summary, it is difficult to find a universal and quantitatively conserved indicator for biogenic emissions in an air mass. Good alternatives, however, are not readily available. Some authors have suggested the use of methanol as a biogenic tracer [*Salisbury et al.*, 2003], but this work will show that primary anthropogenic sources of this VOC are also significant.

3. Results and Discussion

3.1. Removal of Primary Anthropogenic VOCs

[24] The assumption that the sources of anthropogenic VOCs were co-located and that the removal is governed by reactions with OH implies that any two compounds with the same OH rate coefficient must be well correlated. An example is shown in Figure 1a, which shows a scatterplot of benzene ($k = 1.22 \times 10^{-12} \text{ cm}^3 \text{ molecule}^{-1} \text{ s}^{-1}$ [*Atkinson and Arey*, 2003]) versus acetylene ($k = 0.83 \times 10^{-12} \text{ cm}^3 \text{ molecule}^{-1} \text{ s}^{-1}$ [*Sander et al.*, 2002]) color-coded by the photochemical age (equation (1)). The linear

correlation coefficient, r , is 0.96. Figure 1b shows a scatterplot of ethyl benzene ($k = 7.0 \times 10^{-12} \text{ cm}^3 \text{ molecule}^{-1} \text{ s}^{-1}$ [Atkinson and Arey, 2003]) versus acetylene, again color-coded by the photochemical age. The degree of linear correlation is clearly lower than in Figure 1a, and it can be seen that at a high photochemical age the ethyl benzene/acetylene ratio is lower than at a low age. This is easily explained, of course, by the fact that ethyl benzene is removed more efficiently from an air mass than acetylene.

[25] Figures 1c and 1d show the measured benzene/acetylene and ethyl benzene/acetylene ratios versus the photochemical age. As observed above the benzene/acetylene ratio decreases only slowly with photochemical age, whereas the ethyl benzene/acetylene ratio decreases by an order of magnitude over the course of two days. The data in Figures 1c and 1d are described by:

$$\frac{[\text{VOC}]}{[\text{C}_2\text{H}_2]} = ER_{\text{VOC}} \times \exp[-(k_{\text{VOC}} - k_{\text{C}_2\text{H}_2})[\text{OH}]\Delta t], \quad (3)$$

where [VOC] and [C₂H₂] are the volume mixing ratios of a primary VOC (benzene and ethyl benzene in this case) and acetylene, ER_{VOC} is the emission ratio of the VOC versus acetylene, and k_{VOC} and $k_{\text{C}_2\text{H}_2}$ are the rate coefficients for the reactions of those compounds with OH ($3 \times 10^6 \text{ molecules cm}^{-3}$ [Warneke et al., 2004]). The full curves in Figures 1c and 1d show the best fit of equation (3) to the data. The OH rate coefficients from the fits are $(0.97 \pm 0.05) \times 10^{-12} \text{ cm}^3 \text{ molecule}^{-1} \text{ s}^{-1}$ for benzene and $(5.6 \pm 0.2) \times 10^{-12} \text{ cm}^3 \text{ molecule}^{-1} \text{ s}^{-1}$ for ethyl benzene, both about 20% smaller than the literature rate coefficients mentioned above. It should be noted that these results do not depend on the 24-hour averaged OH concentration assumed: if a lower value of [OH] is assumed, then the photochemical age according to equation (1) increases, and the product [OH] Δt in equation (3) remains the same. The emission ratios versus acetylene from the fits are 0.210 ± 0.003 for benzene and 0.108 ± 0.003 for ethyl benzene. The latter value is in excellent agreement with an average, urban ethyl benzene/acetylene ratio of 0.11 reported by Seila et al. [1989] from measurements in 39 U.S. cities. The emission ratio for benzene is lower than the value of 0.33 from Seila et al. [1989]. The reason is probably that benzene emissions from vehicles have systematically decreased over the last decade due to changes in the gasoline formulation [Fortin et al., 2005].

[26] Similar analyses as shown for benzene and ethyl benzene were performed for all primary anthropogenic VOCs measured during NEAQS and the results are summarized in Figures 2 and 3. The emission ratios derived from the NEAQS data are compared in Figure 2 with the average composition of urban air reported by Seila et al. [1989], and with the emission ratios for vehicle exhaust from Harley et al. [1992]. Apart from a few notable exceptions, the hydrocarbon source profile derived from the NEAQS data set agrees very well with the numbers from Seila et al. [1989]. The exceptions included ethane, propane and 2,2,4-trimethyl pentane, which were higher, and n-butane, which was significantly lower during NEAQS. In the case of propane, Sive et al. [2003] also observed enhanced ratios versus other trace gases in New England. The speciation of VOCs in vehicle exhaust is

remarkably similar to that for urban air, in particular for alkenes (Figure 2b) and aromatics (Figure 2c). The emission ratios for the C₂-C₄ alkanes are higher in urban air than in vehicle exhaust, probably because the evaporation of gasoline is an important source of these VOCs [Harley et al., 1992].

[27] Rate coefficients for the reaction with OH were determined for all primary anthropogenic VOCs, and Figure 3 shows the results as a function of the literature values [Atkinson and Arey, 2003]. The blue symbols show the results that were obtained using toluene/benzene and the green symbols using o-xylene/toluene ratios to determine the photochemical age. Rate coefficients for alkenes could only be determined with large uncertainties, because of the small mixing ratios and the very efficient removal, and have been omitted from Figure 3. Using the age from toluene/benzene ratios, there is a reasonable agreement between the literature rate coefficients and the values determined from the NEAQS data set up until the rate coefficient of toluene. At higher rate coefficients the NEAQS values become approximately constant. These findings suggest that the photochemical age determined from toluene/benzene ratios does not give an accurate description of processes that are faster than the removal of toluene. The accuracy of the photochemical age estimate according to equation (1) is limited by (1) the measurement uncertainty of benzene and toluene, and (2) the variation in toluene/benzene emission ratios in space and time. For the more reactive VOCs, the removal time is of the same order as the uncertainty in the photochemical age, and thus the analysis cannot be expected to work well. In addition, due to the mixing between more and less aged air masses, the analysis is expected to be less accurate for more reactive species. The photochemical age was also determined from the measured ratio between o-xylene and toluene, and the analysis was repeated. The results are shown by the green symbols in Figure 3. In this case, there is a good agreement between the literature rate coefficients and the numbers derived from the NEAQS data up until the rate coefficient of o-xylene. At higher values the experimental values also become constant. We will use the photochemical age derived from toluene/benzene ratios in the remainder of the paper. The photochemical age determined from o-xylene/toluene ratios only gives accurate results for the first 24 hours, because o-xylene is typically removed after such a period, and in this work we are interested to follow the time evolution of OVOCs and POM over longer timescales.

[28] Two conclusions from Figures 2 and 3 are pointed out here. First, the mixture of anthropogenic VOC emissions responsible for the pollution observed during NEAQS closely resembled that of an average U.S. city, in particular for aromatic species. Secondly, the photochemical age defined according to equation (1) can be used to describe the evolution of an air mass, but has limitations for reactive processes that are faster than the removal of toluene.

3.2. Production of Alkyl Nitrates

[29] Figure 4 shows a scatterplot of iso-propyl nitrate versus acetylene color-coded by the photochemical age from equation (1). It is seen from Figure 4 that the iso-propyl nitrate/acetylene ratio increases with photochemical age, in contrast with the similar plot for ethyl benzene

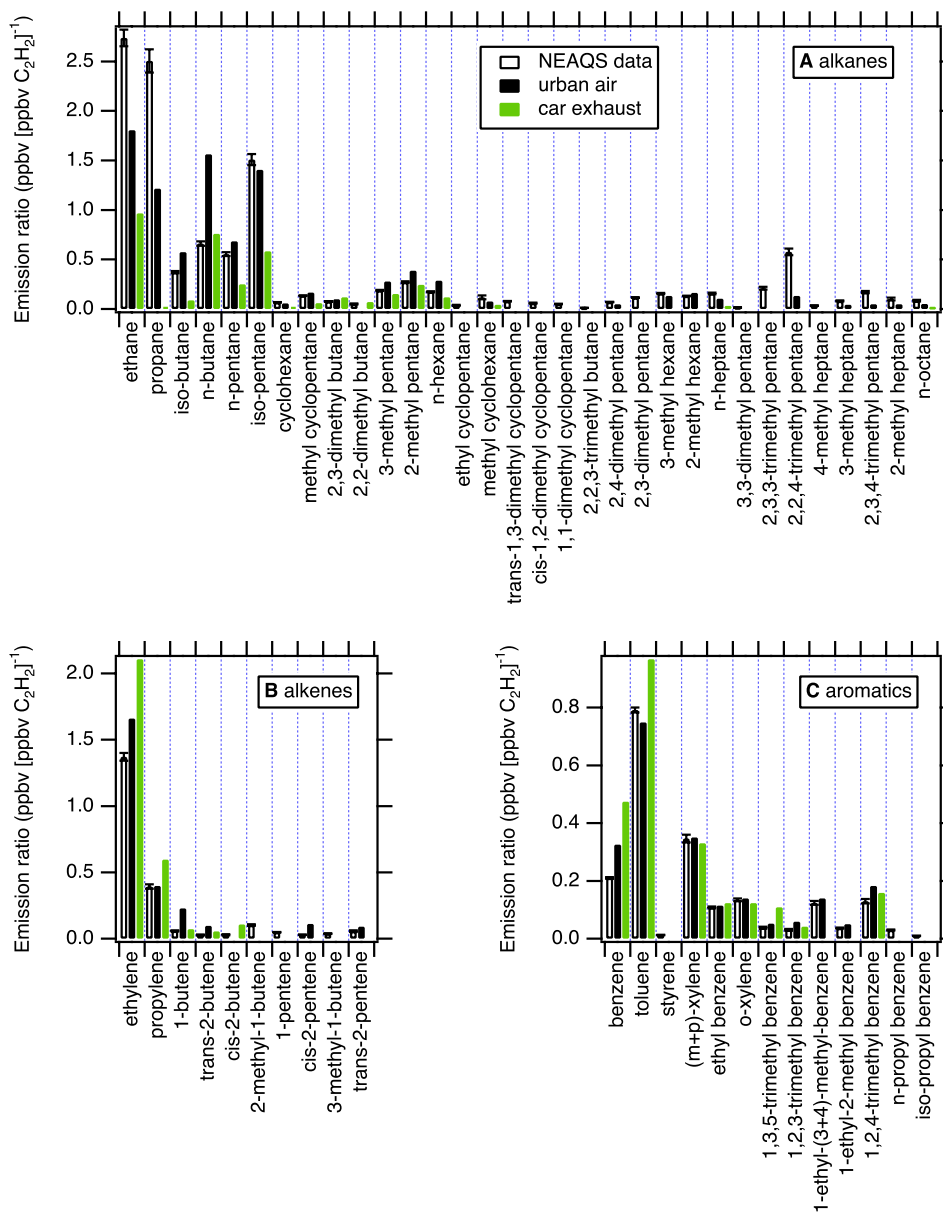


Figure 2. VOC emission ratios derived from the NEAQS data compared with the average composition of urban air [Seila *et al.*, 1989] and car exhaust [Harley *et al.*, 1992].

(Figure 1b). The increase is easily explained by the fact that iso-propyl nitrate has no direct emission sources and is formed in the atmosphere from the oxidation of propane and other anthropogenic VOCs. Figure 4b shows the iso-propyl nitrate/acetylene ratio versus photochemical age, and the ratio increased by almost an order of magnitude over the course of two days.

[30] The data in Figure 4b can be described by:

$$\frac{[\text{AN}]}{[\text{C}_2\text{H}_2]} = Y_{\text{AN}} \times ER_{\text{precursor}} \times \frac{k_{\text{precursor}}}{k_{\text{AN}} - k_{\text{precursor}}} \times \frac{\exp(-k_{\text{precursor}}[\text{OH}]\Delta t) - \exp(-k_{\text{AN}}[\text{OH}]\Delta t)}{\exp(-k_{\text{C}_2\text{H}_2}[\text{OH}]\Delta t)}, \quad (4)$$

where [AN] is the mixing ratio of the alkyl nitrate, $ER_{\text{precursor}}$ is the emission ratio versus acetylene of the

precursor for iso-propyl nitrate, Y_{AN} is the alkyl nitrate yield from that precursor, and $k_{\text{precursor}}$ and k_{AN} are the OH rate coefficients for the precursor and the alkyl nitrate, respectively. The full curve in Figure 4b shows the result of fitting equation (4) to the data using the following parameters: $ER_{\text{precursor}} = 2.5$ (found for propane during NEAQS; Figure 2), $k_{\text{precursor}} = 1.09 \times 10^{-12} \text{ cm}^{-3} \text{ molecule}^{-1} \text{ s}^{-1}$ (propane) [Atkinson and Arey, 2003] and $k_{\text{AN}} = 5 \times 10^{-13} \text{ cm}^{-3} \text{ molecule}^{-1} \text{ s}^{-1}$ (for iso-propyl nitrate including a term due to photolysis) [Roberts, 1990]. The only parameter that was varied was Y_{AN} and the best fit was obtained for a yield of 3.8%. This number is somewhat larger than the literature value of 2.9% (from the Master Chemical Mechanism v2.0 described by Jenkin *et al.* [1997]). The reason for the difference is probably that there are more precursors for iso-propyl nitrate than just propane. This observation agrees with the work of Bertman *et al.*

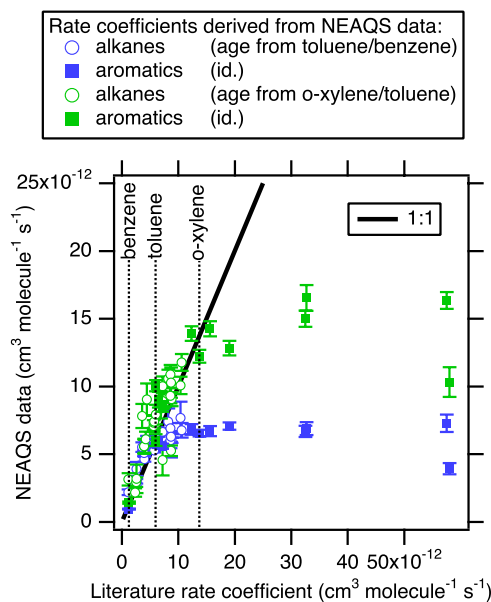


Figure 3. Comparison between the rate coefficients for alkanes and aromatics derived from the NEAQS data set and those from the literature [Atkinson and Arey, 2003].

[1995], who noted that the levels of iso-propyl radicals in the atmosphere are up to 50% higher than can be accounted for from propane oxidation, due to thermal decomposition of longer-chain alkoxy radicals.

[31] In Figure 5 the time series of iso-propyl nitrate calculated from equation (4) is compared with the measurements. The time series for acetylene and the photochemical age (Δt) that are used in the calculation are shown in Figure 5a for part of the NEAQS data. There is a weak anti-correlation between acetylene and the photochemical age: when the age is low, the ship was sampling close to sources and the acetylene mixing ratio is high. There were also instances, however, when acetylene and the photochemical age were both high, and these are exactly the conditions when iso-propyl nitrate showed its highest mixing ratios. The measured time series for iso-propyl nitrate is compared with the calculation in Figure 5b for part of the NEAQS study period. Figure 5c contains a scatterplot of calculated versus measured iso-propyl nitrate for the entire NEAQS data set. We conclude that the fit describes much of the variability observed for iso-propyl nitrate. It should be noted that the fit shown in Figure 5b is based on chemical kinetics, on the measurements of three species (acetylene, benzene and toluene), the emission ratio of propane, and contains only one adjustable parameter for the whole data set: the yield of iso-propyl nitrate from the oxidation of propane and other VOCs.

3.3. Sources and Chemistry of OVOCs

[32] In the preceding two sections it has been shown that the removal of primary anthropogenic VOCs and the production of alkyl nitrates can be well described using the analysis developed in this work. In case of the OVOCs the chemistry and emissions are more uncertain and it will be assumed that they have both primary and secondary anthropogenic sources. In addition, some OVOCs have

biogenic sources, which will be assumed to be proportional to the parameter isoprene_{source} as introduced in section 2.2. The measured OVOC mixing ratios will be described by:

$$\begin{aligned}
 [\text{OVOC}] = & ER_{\text{OVOC}} \times [\text{C}_2\text{H}_2] \times \exp(-k_{\text{OVOC}} - k_{\text{C}_2\text{H}_2})[\text{OH}]\Delta t \\
 & + ER_{\text{precursor}} \times [\text{C}_2\text{H}_2] \times \frac{k_{\text{precursor}}}{k_{\text{OVOC}} - k_{\text{precursor}}} \\
 & \times \frac{\exp(-k_{\text{precursor}}[\text{OH}]\Delta t) - \exp(-k_{\text{OVOC}}[\text{OH}]\Delta t)}{\exp(-k_{\text{C}_2\text{H}_2}[\text{OH}]\Delta t)} \\
 & + ER_{\text{biogenic}} \times (\text{isoprene}_{\text{source}}) + [\text{background}]. \quad (5)
 \end{aligned}$$

The first term represents the removal of the primary anthropogenic OVOC emissions similarly to equation (3). The second term represents the production and removal of secondary anthropogenic OVOCs and is similar to equation (4). The OVOC yield is assumed to be equal to 1 in equation (5), since the yield and emission ratio cannot be determined independently from the regression. The third term represents the biogenic contribution to the OVOCs, and the fourth term the OVOC mixing ratio in background conditions. The parameters k_{OVOC} are taken from Atkinson and Arey [2003], whereas $k_{\text{precursor}}$, ER_{OVOC} , $ER_{\text{precursor}}$, ER_{biogenic} and [background] are determined from a linear least-squares fit that minimizes the difference between the

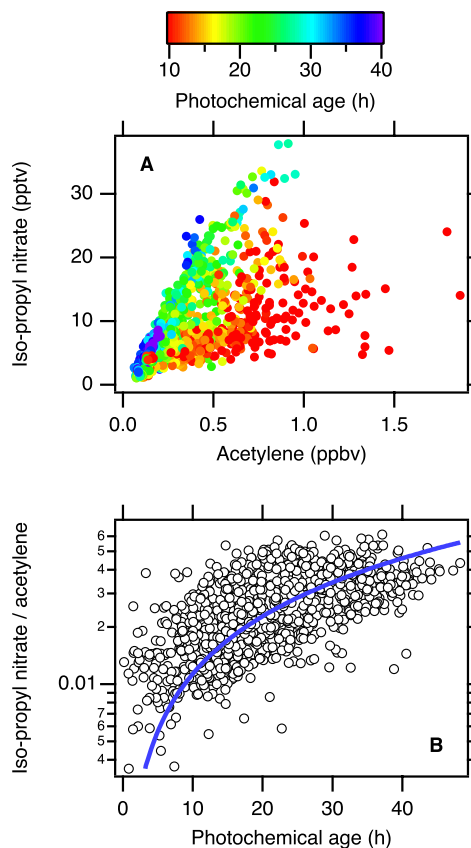


Figure 4. Scatterplot of iso-propyl nitrate versus acetylene. (a) Scatterplot color-coded by the photochemical age derived from measured benzene/toluene ratios. (b) Iso-propyl nitrate/acetylene ratio versus the photochemical age along with the result of a fit of equation (4) to the data.

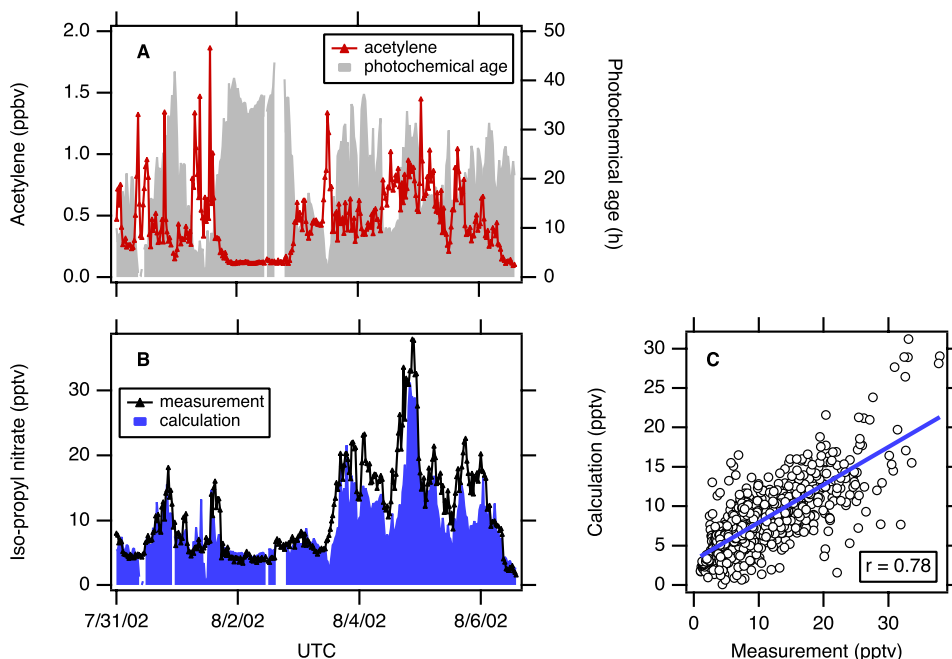


Figure 5. Results of the analysis for iso-propyl nitrate. (a) Acetylene and the photochemical age that are used in the fit. (b) Comparison of the measured and calculated iso-propyl nitrate mixing ratio for part of the study period. (c) Scatterplot of the calculated versus the measured values for the entire NEAQS data set.

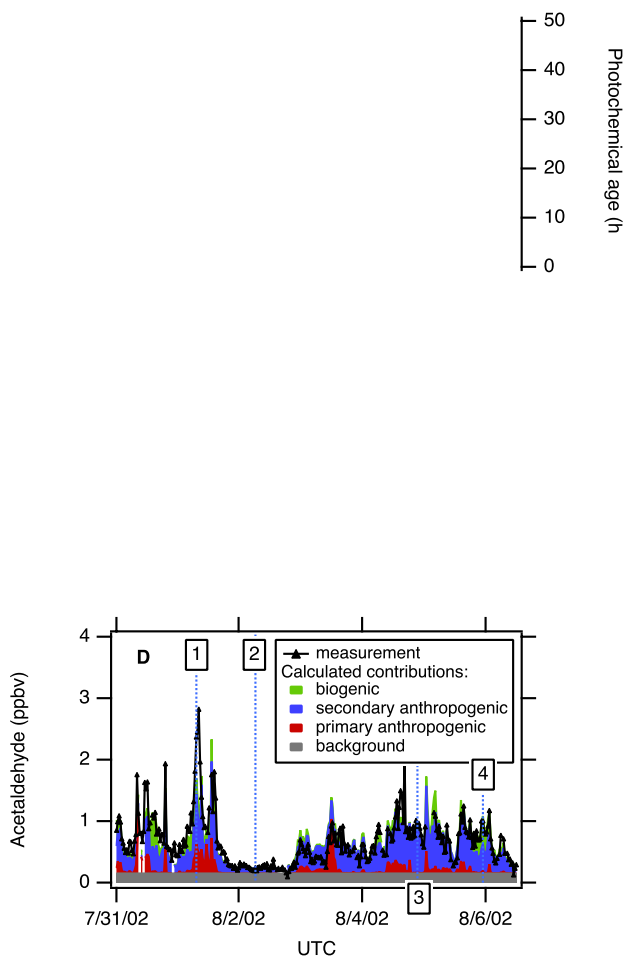
measured OVOC mixing ratios and those calculated from equation (5).

[33] The third term in equation (5) gives only a semi-quantitative description of the biogenic contribution. Formally, the biogenic contribution should be described similarly to the anthropogenic terms in equation (5) by adding a primary contribution that is removed exponentially in time, and a secondary contribution that increases and then decreases with time. However, the biogenic contribution to most organic species studied in this work was found to be only small, as will be seen below, and the results did not justify describing the biogenic contribution in equation (5) with the same level of detail as the anthropogenic contribution. The parameter $ER_{biogenic}$ should be regarded as an empirical parameter that describes the enhancement ratio of an OVOC relative to $isoprene_{source}$ after a processing time of about 3 hours, i.e. the average processing time of biogenic emissions at the time the ship sampled the air. Also, the description does not allow separating the primary biogenic and secondary biogenic contributions.

[34] The result of the analysis for acetaldehyde is shown in Figure 6. Figure 6a shows the measured acetylene mixing ratio, and the values determined for the photochemical age that are used in the calculation. Figure 6b shows the measured mixing ratios of isoprene and the sum of MVK and MACR, as well as the parameter $isoprene_{source}$ calculated using the reactions in equation (2). Figure 6c shows a scatterplot of $isoprene_{source}$ versus $MVK + MACR$ color-coded by the processing time estimated from the reactions in equation (2). It is seen that at low processing times, the parameter $isoprene_{source}$ is well correlated with $MVK + MACR$, where the slope is determined by the yield of $MVK + MACR$ from the reaction between OH and

isoprene (54%). At higher processing times, the parameter $isoprene_{source}$ is calculated to be higher than $(MVK + MACR)/0.54$ as a result of the finite lifetimes of MVK and MACR themselves. For these air masses the value of $isoprene_{source}$ is obviously an extrapolation and therefore uncertain, although Figure 6c shows that the extrapolation is never more than a factor of 2–3. Figure 6d shows the result of fitting equation (5) to the measured acetaldehyde data for part of the NEAQS data set; the different colors represent the four different terms of equation (5). Figure 6e shows the comparison between the measured and calculated acetaldehyde mixing ratios for the entire NEAQS data set. The parameters that best described the measured data are given in Table 1. The error estimates in Table 1 were obtained from the regression analysis and were small for the parameters ER_{OVOC} , $ER_{biogenic}$ and [background]. The underlying reason is that the degree of linear correlation between the data for acetylene and $isoprene_{source}$ was small (r was 0.30 for the data shown in Figure 6, and 0.53 for the whole data set), and mostly driven by the clean periods such as on August 2nd and 3rd when no anthropogenic and biogenic influences were detected. It is seen from Figure 6d that most of the acetaldehyde was secondary from anthropogenic sources, with smaller primary anthropogenic and biogenic contributions. Table 2 shows what percentage of acetaldehyde measured during the entire NEAQS period was attributed to the different sources.

[35] Figure 7 gives some examples of back-trajectories for the air masses sampled on the Ronald H. Brown. From the data in Figure 5 and 6, four points in time were chosen that showed, respectively, a high primary anthropogenic contribution (time 1 in Figure 6d), clean marine air (time 2), a high secondary anthropogenic contribution (time 3), and a



high biogenic contribution (time 4). For these 4 points in time back-trajectories were calculated and the results are shown in Figure 7. Due to the complex meteorology in the coastal zone, the transport of continental air to the marine boundary layer, and vice versa, is difficult to describe, and the trajectories in Figure 7 should be treated with some

caution [Angevine *et al.*, 2004]. Nevertheless, the trajectories clearly show the types of air masses sampled by the ship. Around time 1, the air masses came straight from the Portsmouth area during the night and early morning. This episode, also described by Goldan *et al.* [2004], showed some of the highest loadings of reactive anthropogenic

Table 2. Linear Correlation Coefficient (r) for the Measured and Calculated OVOC Mixing Ratios, and the Percentages of OVOCs Attributed to Different Sources

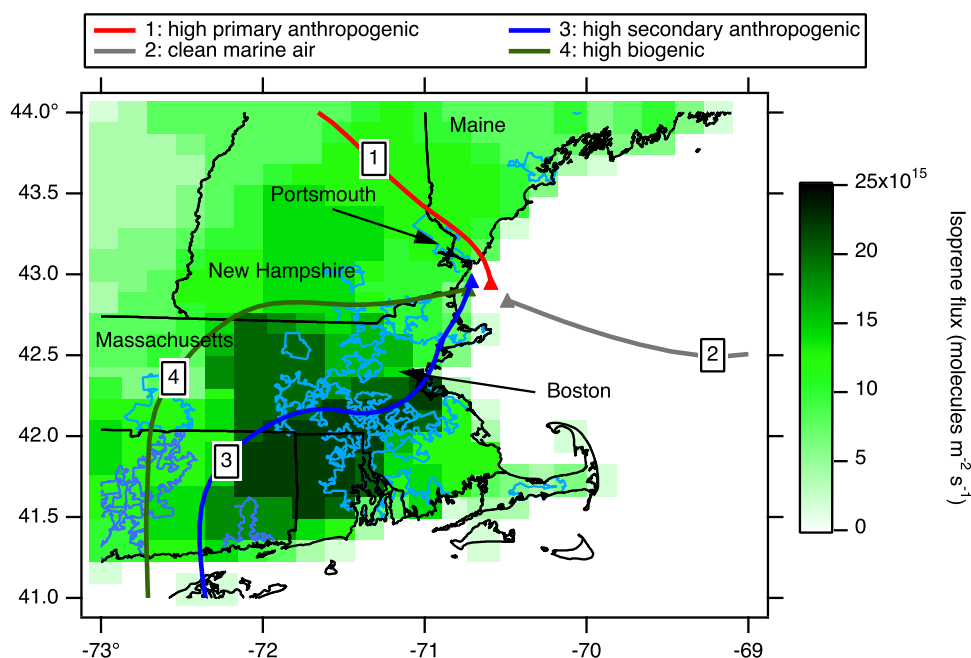
Compound	r	Primary		Secondary		Biogenic, %	Background, %
		Anthropogenic, %	Anthropogenic, %	Anthropogenic, %	Anthropogenic, %		
Acetaldehyde	0.89	9	51	13	26		
Propanal	0.77	9	62	10	19		
Acetone	0.79	25	16	13	46		
MEK	0.87	48	17	19	16		
Methanol	0.73	33	0	20	48		
Ethanol	0.68	69	0	7	24		
Formic acid	0.75	0	53	33	14		
Acetic acid	0.76	2	59	29	10		
PAN	0.65	0	75	25	0		
PPN	0.67	0	97	3	0		
PiBN	0.65	0	98	2	0		
MPAN	0.78	0	14	86	0		

hydrocarbons. Around time 2, the ship sampled relatively clean air for about two days. Figure 7 shows that the air masses came from the East during this period. At time 3, the ship sampled some of the highest loadings of secondary anthropogenic species such as iso-propyl nitrate (see also Figure 5). During this period the ship was located near the coast of New Hampshire and sampled air from the Boston, Massachusetts, area that had been processed for approximately one day. Finally, at time 4 the ship sampled air that had mostly traveled over rural areas around the New Hampshire-Massachusetts border, and contained high levels of isoprene and its photoproducts.

[36] Similar analyses as shown for acetaldehyde in Figure 6 were performed for all the other OVOCs measured during NEAQS, and the results are shown in Figure 8 and in Tables 1 and 2. Similarly to acetaldehyde most of the propanal was attributed to secondary anthropogenic sources. The two ketones, acetone and methyl ethyl ketone (MEK),

are mostly attributed to primary anthropogenic sources with smaller contributions from secondary anthropogenic and biogenic sources. The two alcohols, methanol and ethanol, have significant primary anthropogenic but negligible secondary anthropogenic sources. For methanol a significant biogenic contribution is inferred from the NEAQS data. The two acids are attributed to secondary anthropogenic and biogenic sources, with a negligible contribution from primary anthropogenic sources. For all species the values for the background term in equation 5 (Table 1) are mostly determined by the mixing ratios observed in clean marine conditions, such as on August 2nd and 3rd (see Figure 8).

[37] The primary anthropogenic emission ratios derived in this work are compared with literature values in Table 3. *Li et al.* [1997] reported OVOC emission ratios downwind of Vancouver and their results are in reasonable agreement with the values presented here. Several authors have shown that carbonyl emissions from vehicles are low relative to

**Figure 7.** Back-trajectories for some of the main features in Figure 6. The triangles show the ship's location, the colored background gives the isoprene emissions, and the light blue outlines show the location of the main urban centers.

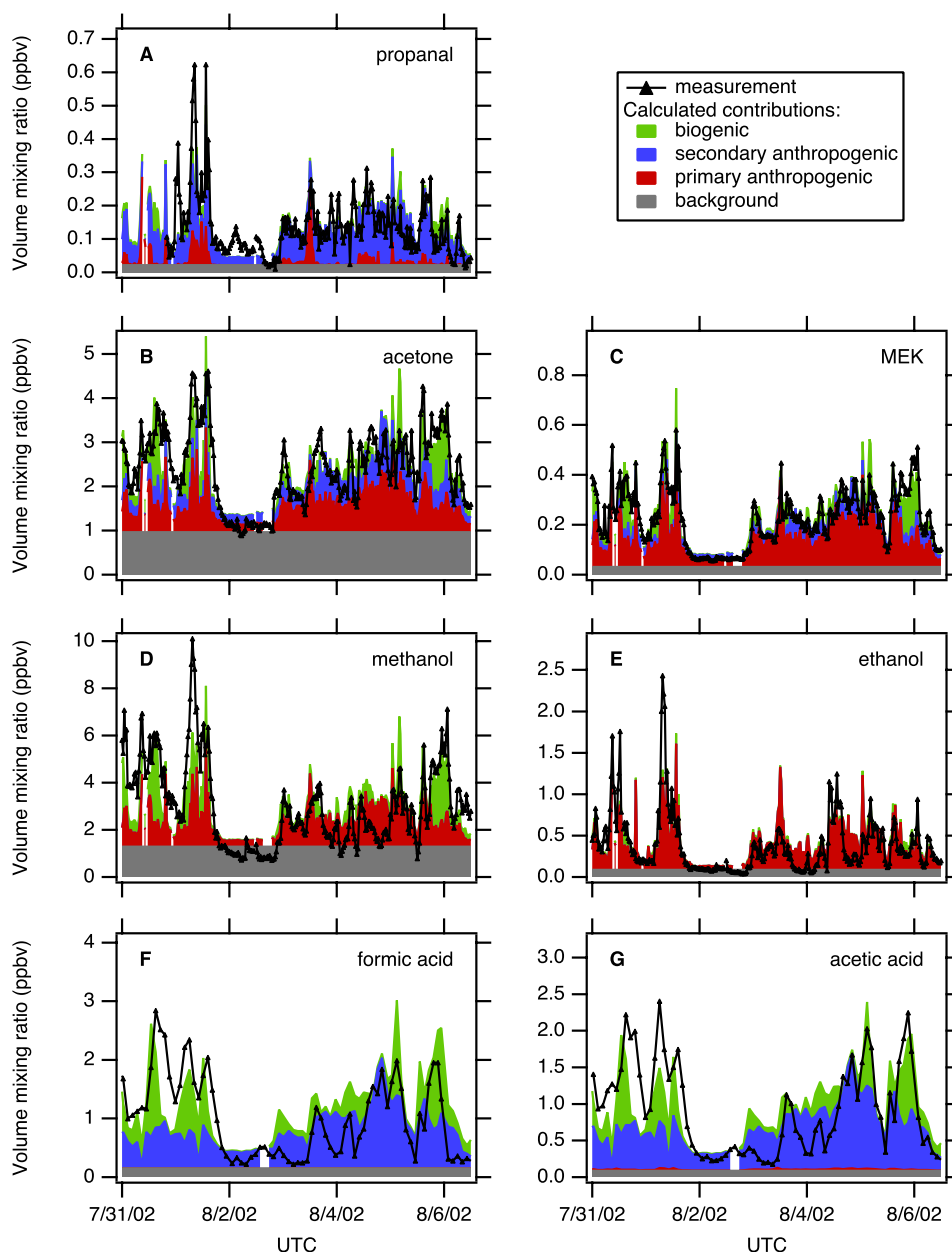


Figure 8. Results of the analysis for all OVOCs measured during NEAQS for part of the study period.

emissions of aromatic hydrocarbons [Harley *et al.*, 1992; Grosjean *et al.*, 2001; Kristensson *et al.*, 2004]. The presently found emission ratios of OVOCs are much higher, suggesting that vehicles are not the dominant sources of OVOCs in urban areas. OVOC emissions from diesel trucks were found to be much higher than those from gasoline vehicles (Table 3) [Schauer *et al.*, 1999, 2002a]. Nevertheless, the contribution from diesel trucks to the total vehicle emissions is relatively small in the U.S. (4% [Kirchstetter *et al.*, 1999]), which means that OVOC emission ratios averaged over the entire fleet will be close to those for gasoline-powered vehicles. Larger sources of OVOCs may include their use as solvent in coatings and adhesives [Harley *et al.*, 1992]. It is also possible that the vegetation in cities, which is typically different from the surrounding areas, contributes to the emissions of species like methanol.

[38] Several authors have studied biogenic emissions of OVOCs in recent years [MacDonald and Fall, 1993; Fukui and Doskey, 1998; Kirstine *et al.*, 1998; Baker *et al.*, 2001; Schade and Goldstein, 2001]. A flux study at the Prophet research site in Michigan by Karl *et al.* [2003] seems appropriate for comparison with the present data: the forest types in both northern Michigan and New England were characterized as northern mixed and northern coniferous by Geron *et al.* [2000]. The results from Karl *et al.* [2003] are contrasted to those of the present study in Table 4. It is seen that there is a good agreement between the two data sets. The emission ratios for acetaldehyde and methanol derived from the NEAQS data are in the range of values observed by Karl *et al.* [2003], whereas the emission ratio for acetone is slightly higher. The parameterization of the biogenic contribution to OVOC concentrations is one of the more

Table 3. Ratio Between Urban Emissions of OVOCs and Acetylene^a

Compound	This Work	Li ^{b,c}	Harley ^d	Kristensson ^{c,e}	Schauer ^f	Schauer ^g
Acetaldehyde	0.83 ± 0.07		0.14	0.076	0.18	5.4
Propanal	0.24 ± 0.02	0.40	0.01		0.022	1.4
Acetone	1.2 ± 0.2	1.9	0.07	0.026	0.042	2.1
MEK	0.26 ± 0.02	0.36	0.01	0.009	0.013	0.6

^aUnits are in ppbv [ppbv C₂H₂]⁻¹.

^bUrban air, Vancouver, Canada [Li *et al.*, 1997].

^cAssuming a C₂H₂/CO emission ratio of 4.94 pptv ppbv⁻¹.

^dVehicle exhaust, Los Angeles, California [Harley *et al.*, 1992].

^eTunnel study, Sweden [Kristensson *et al.*, 2004].

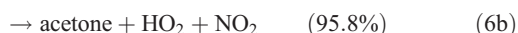
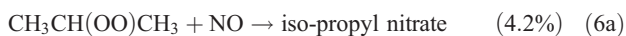
^fGasoline-powered motor vehicles [Schauer *et al.*, 2002a].

^gMedium duty diesel trucks [Schauer *et al.*, 1999].

uncertain elements in the analysis presented here. As discussed in section 2.2, isoprene is not a very suitable indicator for biogenic emissions due to its high reactivity and the importance of nighttime reactions with NO₃. The agreement between the OVOC emission ratios reported by Karl *et al.* [2003] and the present results is therefore encouraging, but should be treated with some caution.

[39] Biogenic emissions of organic acids from several tree and crop species were studied by Kesselmeier *et al.* [1997, 1998] and were generally found to be small. Consequently, the biogenic contributions relative to isoprene for both formic and acetic acid (Table 1) are probably due to secondary production from biogenic precursors rather than direct emissions. The results of the analysis suggest that biogenic sources accounted for an average of about 30% of these compounds (Table 2), which is relatively low compared to other studies. For example, radiocarbon analyses suggest that biogenic sources contribute 55% to 64% of formic and acetic acid in urban air in Milan, Italy, with even higher contributions at less-polluted rural locations [Glasius *et al.*, 2001]. Comparisons between absolute and relative wet-deposition fluxes of formic and acetic acids in polluted and remote regions of the world support the hypothesis that biogenic precursors are the dominant sources in nonurban industrialized regions of eastern North America [e.g., Keene and Galloway, 1988]. The possibility exists that the analysis used here does not properly distinguish between secondary formation from biogenic and anthropogenic precursors, and this is investigated in more detail in the next section.

[40] Recently Jacob *et al.* [2002] described the global, atmospheric budget of acetone and found that the dominant secondary anthropogenic source is from propane and iso-alkane oxidation. Multiplying the emission ratios of propane, iso-butane and iso-pentane from Figure 2 with the acetone formation yields from Jacob *et al.* [2002], gives a value for $ER_{precursor}$ of 3.0 ± 0.2 ppbv [ppbv C₂H₂]⁻¹, which is somewhat higher than the precursor emission ratio of 1.7 ± 0.6 ppbv [ppbv C₂H₂]⁻¹ determined by the fit (Table 1). Both acetone and iso-propyl nitrate are formed from the reaction between the CH₃CH(OO)CH₃ peroxy radical with NO [Jenkin *et al.*, 1997]:



Using the results from the fit shown in Figures 5b and 8b, we can estimate the ratio between the atmospheric

formation of iso-propyl nitrate and acetone, and the result is $5 \pm 2\%$ in agreement with the ratio of 4.2% expected from the kinetics (equation (6a)) [Jenkin *et al.*, 1997]. Primary anthropogenic emissions of acetone, primarily from vehicle exhaust, were assumed to be small in the budget of Jacob *et al.* [2002].

[41] Several authors have discussed the global, atmospheric budget of methanol [Galbally and Kirstine, 2002; Heikes *et al.*, 2002]. Unlike the findings from NEAQS (Table 2), biogenic emissions are the dominant source of methanol to the global atmosphere in these budgets. Of course, the NEAQS study area was heavily impacted by pollution sources in the northeastern U.S. and is not representative for the global atmosphere. The second important source of methanol is atmospheric formation from methane. However, this process is too slow to produce significant methanol in two days and in addition only occurs at low levels of NO_x [Jenkin *et al.*, 1997], which may explain why secondary formation was not inferred from the NEAQS data. Much of the methanol observed during NEAQS is attributed to the background and may be from methane oxidation.

[42] Acetaldehyde and propanal were both determined to be mostly secondary anthropogenic during NEAQS. In the case of acetaldehyde, this observation is in qualitative agreement with the work of Harley and Cass [1994]. For both acetaldehyde and propanal the emission ratios of their precursors were suggested to be high from the fit: 6.9 ± 0.9 ppbv [ppbv C₂H₂]⁻¹ for acetaldehyde and 3 ± 1 ppbv [ppbv C₂H₂]⁻¹ for propanal. Ethane, n-butane, iso-pentane and propylene are all efficient precursors for acetaldehyde [Jenkin *et al.*, 1997]. Multiplying their emission ratios from Figure 2 with the acetaldehyde yields from Carter [1990] gives an estimate for $ER_{precursor}$ of 4.6 ppbv [ppbv C₂H₂]⁻¹, i.e. about 30% smaller than the value of 7 ± 1 ppbv [ppbv C₂H₂]⁻¹ determined from the fit. In addition, the reaction of C_n-aldehydes with OH in the presence of NO_x leads in part

Table 4. Ratio Between Biogenic Emissions of OVOCs and Isoprene^a

Compound	This Work	Prophet, Mean ^b	Prophet, Maximum ^b
Acetaldehyde	0.063 ± 0.004	0.06	0.14
Acetone	0.23 ± 0.01	0.08	0.19
Methanol	0.44 ± 0.02	0.23	0.55

^aUnits are in ppbv [ppbv isoprene]⁻¹.

^bData from the Prophet research site [Karl *et al.*, 2003]. The mean values refer to the seasonal mean, and the maximum values refer to the daytime high.

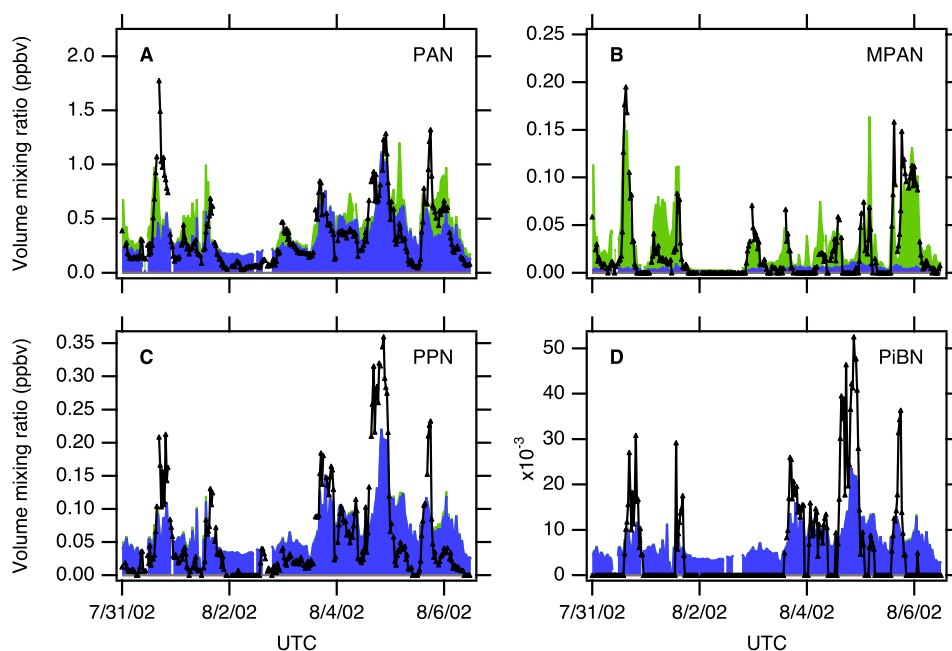


Figure 9. Results of the analysis for all PANs measured during NEAQS for part of the study period. The symbols are the same as in Figure 8.

to the formation of C_{n-1} -aldehydes [Atkinson and Arey, 2003]. These observations show that there is an efficient mechanism for sustained production of aldehydes in the atmosphere, a conclusion that is corroborated by the observation of these species in background tropospheric conditions [Singh *et al.*, 2001, 2003].

3.4. Sources of Peroxyacyl Nitrates

[43] The ability of the analysis developed in this work to quantitatively separate anthropogenic and biogenic sources was tested by performing the same analysis for four different PAN compounds measured during NEAQS. The percentages attributed to the different sources for the entire NEAQS data set are shown in Table 2. PPN and PiBN are known to be formed from the oxidation of anthropogenic precursors [Williams *et al.*, 1997; Roberts *et al.*, 2002], and are almost exclusively attributed to secondary anthropogenic sources by the fit (97% and 98%, respectively). MPAN, on the other hand, is formed from the oxidation of isoprene, and is here mostly attributed to biogenic sources (86%) with a minor contribution from secondary anthropogenic sources (14%). Figure 9 shows the results of the analyses of PAN species for the same sampling period as in Figures 6 and 8. It is seen that in particular the data for PAN and MPAN are well described by equation (5). The time series for PPN and MPAN are very dissimilar ($r = 0.05$ for the period in Figure 9), and MPAN is almost entirely attributed to biogenic and PPN to secondary anthropogenic sources.

[44] Several authors have described the traffic-related sources of isoprene and of methacrolein, the direct precursor of MPAN, in urban air [Borbon *et al.*, 2001; Biesenthal and Shepson, 1997]. However, the emission ratios are generally found to be small, and may not be enough to account for the 14% of MPAN attributed to secondary anthropogenic sources. To further evaluate the sensitivity of these results, we conducted a second set of calculations using iso-propyl

nitrate as the tracer of secondary anthropogenic sources. This formulation attributed a larger percentage (32%) of MPAN to secondary anthropogenic sources. Both sets of results suggest the possibility that our analysis may misallocate finite fractions of secondary biogenic sources to secondary anthropogenic sources. The formation of MPAN requires the presence of NO_x in addition to isoprene, and MPAN is therefore expected to be higher in polluted air than in clean air that has been exposed to the same biogenic emissions. As a result, the method used in this work will attribute part of the MPAN to anthropogenic sources even though the hydrocarbon part of the molecule is biogenic. A similar uncertainty in distinguishing secondary anthropogenic from secondary biogenic sources may exist for the OVOCs investigated in the previous section, and the POM studied in the next.

[45] PAN is known to have anthropogenic and biogenic precursors [Williams *et al.*, 1997], and the analysis indeed shows a contribution from secondary anthropogenic (75%) and biogenic (25%) sources. These numbers agree well with a study in Nashville, where on average 80% of the PAN and thus ozone was attributed to anthropogenic and 20% to biogenic precursors [Roberts *et al.*, 2002]. A more detailed discussion of the PAN data is beyond the scope of this work and will be presented elsewhere.

3.5. Particulate Organic Matter

[46] Figure 10a shows a scatterplot of the sub- μm POM, measured by AMS, versus acetylene, measured by GC-MS during NEAQS. The data points are color-coded by the photochemical age determined from equation (1). The highest ratios between sub- μm POM and acetylene were observed in air masses with a relatively high photochemical age, whereas the ratio between sub- μm POM and acetylene was low in air masses that are photo-chemically “young”. The gray area in Figure 10a shows the range of POM/

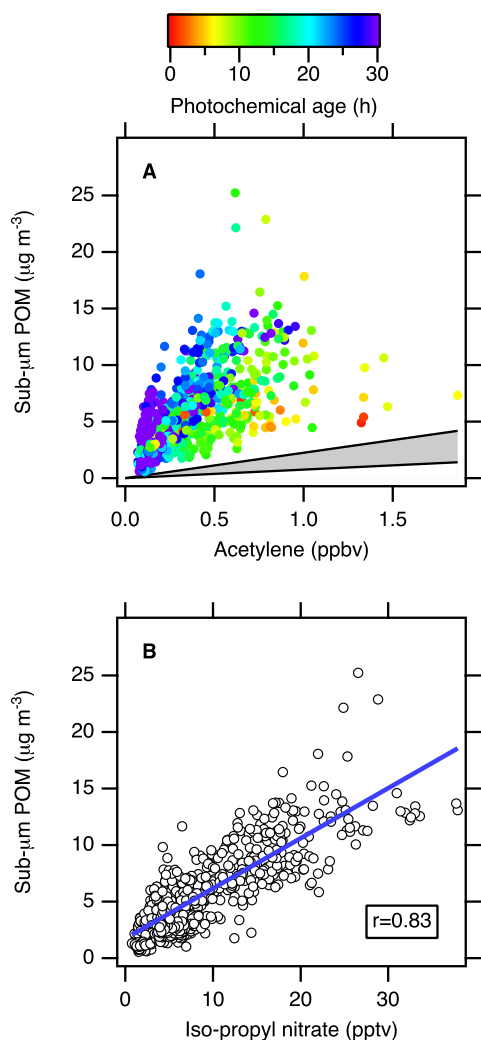


Figure 10. Scatterplots of the sub- μm POM measured during NEAQS versus (a) acetylene and (b) iso-propyl nitrate. The gray area in Figure 10a shows the range of ratios between sub- μm POM and acetylene observed by *Kirchstetter et al.* [1999] in urban air.

acetylene ratios that have been observed in urban air by *Kirchstetter et al.* [1999] (using an acetylene/CO ratio of $4.94 \text{ pptv ppbv}^{-1}$). The data points from NEAQS are consistently above the gray area. Figure 10b shows a scatterplot of sub- μm POM versus iso-propyl nitrate, and the linear degree of correlation was high ($r = 0.83$). These observations suggest that a significant fraction of the sub- μm POM measured during NEAQS was secondary anthropogenic, and that the formation took one day or more.

[47] An attempt was made to describe the POM data using the same methodology as described above for the OVOCs, and the results are shown in Figure 11. In applying equation (5) to the description of POM, it should be noted that the loss of POM is not governed by reactions with OH, i.e. the term $k_{\text{OVOC}}[\text{OH}]\Delta t$ in equation (5) should be replaced by $L_{\text{POM}}\Delta t$, where L_{POM} describes the loss of POM. In addition, the units of POM and OVOCs are different, and thus the units of ER_{POM} , $ER_{\text{precursor}}$ and ER_{biogenic} are also different when describing POM using

equation (5). Figures 11a and 11b show that the measured POM data can be reasonably well described by a fit of equation (5). Averaged over the whole NEAQS data set, the dominant fraction of POM was attributed to secondary anthropogenic formation (57%), with smaller contributions from primary anthropogenic (11%) and biogenic (12%) sources. The remaining 21% could not be attributed to any of these sources. The emission ratios for POM from primary anthropogenic and biogenic sources were determined to be $1.9 \pm 1.0 \mu\text{g m}^{-3} [\text{ppbv C}_2\text{H}_2]^{-1}$ and $0.56 \pm 0.06 \mu\text{g m}^{-3} [\text{ppbv isoprene}]^{-1}$, respectively. The other free parameters in equation (5), $ER_{\text{precursor}}$ and the loss rates for POM and its precursors, are coupled in the fit and could not be accurately determined.

[48] The primary anthropogenic POM emission ratio from the fit can be directly compared to the emission ratios obtained from tunnel studies [*Kirchstetter et al.*, 1999] as well as from dynamometer studies of diesel and gasoline fueled vehicles [*Schauer et al.*, 1999, 2002a]. From the work of *Kirchstetter et al.* [1999] and a $\text{C}_2\text{H}_2/\text{CO}$ emission ratio of $4.94 \text{ pptv ppbv}^{-1}$, we estimate the POM emission ratio to be $0.43 \mu\text{g m}^{-3} [\text{ppbv C}_2\text{H}_2]^{-1}$, which is clearly lower than the ratio of $1.9 \pm 1.0 \mu\text{g m}^{-3} [\text{ppbv C}_2\text{H}_2]^{-1}$ determined from the NEAQS data set. From the work of *Schauer et al.* [1999] it is clear that the average POM emission ratio in a region must be highly dependent on the fraction of diesel vehicles: the POM to acetylene emission ratio was measured to be $11 \mu\text{g m}^{-3} [\text{ppbv C}_2\text{H}_2]^{-1}$ for diesel vehicles, whereas it is only $0.25 \mu\text{g m}^{-3} [\text{ppbv C}_2\text{H}_2]^{-1}$ for catalyst-equipped gasoline vehicles. During the tunnel study of *Kirchstetter et al.* [1999], the number of diesel vehicles was determined to be 4% for the Caldecott tunnel between San Francisco and Oakland, California. A higher fraction of diesel vehicles in New England could explain, at least in part, the higher POM emission ratio inferred from the NEAQS data. Finally, it is interesting to note that in background, urban conditions ($\sim 1 \text{ ppmv CO}$), *Kirchstetter et al.* [1999] measured ratios of POM versus acetylene ranging from 0.8 to $2.2 \mu\text{g m}^{-3} [\text{ppbv C}_2\text{H}_2]^{-1}$, i.e. in much better agreement with the value of $1.9 \pm 1.0 \mu\text{g m}^{-3} [\text{ppbv C}_2\text{H}_2]^{-1}$ determined here.

[49] The AMS measurements not only give the mass loading of sub- μm POM, but can also contain information on the degree of chemical processing. In particular, the AMS signal at 44 amu (CO_2^+) has been found to increase from 2.5% of the total signal for nonprocessed organic aerosol to 16% for aerosol that has been processed [*Alfarra et al.*, 2004]. A similar observation was made during NEAQS, although the samples with a ratio as low as 2.5% were limited to those isolated instances when the exhaust from the *Ronald H. Brown* itself was sampled. In Figure 11c the secondary anthropogenic fraction of the sub- μm POM estimated using equation (5) (the second term divided by the total) is compared with the fraction of the total AMS sub- μm POM signal at 44 amu. The two parameters are correlated for much of the period shown in Figure 11c. This means that the larger the secondary fraction of the sub- μm POM, the more processed the particles were according to the AMS measurement. This agrees with expectations and provides some additional justification for the analysis developed in this work.

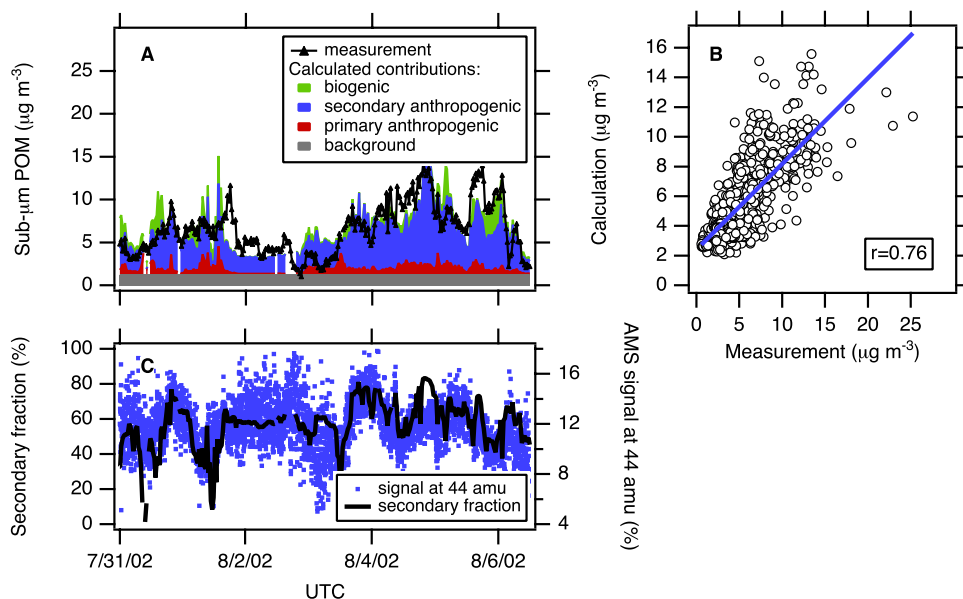


Figure 11. Result of the analysis for the sub- μm POM measured during NEAQS.

[50] Our findings about the relatively small contributions from primary anthropogenic and biogenic sources in the New England region may be surprising. For example, *Rogge et al.* [1996] in a series of papers measured and modeled the emissions of primary organic aerosols in an urban air shed from a variety of sources such as vehicles, road dust, meat cooking, roofing operations, cigarette smoke, domestic fireplaces and leaf abrasion products. In addition, *Schauer et al.* [1996, 2002b] developed a chemical mass balance receptor model for source apportionments of POM, and attributed a large fraction of POM to primary sources (85% in the Los Angeles area). Many authors have studied the secondary formation of POM from biogenic precursors [*Seinfeld and Pandis*, 1998; *Limbeck et al.*, 2003; *Claeys et al.*, 2004], and radiocarbon analyses of POM have indicated relatively high fractions of “modern”, biogenic carbon [e.g., *Klinedinst and Currie*, 1999]. Two examples are shown in the following two paragraphs to strengthen our case that primary anthropogenic and biogenic sources of POM were relatively small in New England.

[51] Figure 12 shows measurement results from a part of the NEAQS study, when the *Ronald H. Brown* was sampling air that came straight from Boston. Figure 12a shows a map of the area along with the ship track, which is color-coded by the measured mixing ratio of toluene. In addition, the arrows show the wind direction. Not surprisingly, it is seen that the highest mixing ratios of toluene were observed when the air came straight from Boston. Figure 12b shows the measurement results for toluene, benzene and sub- μm POM for the period shown in Figure 12a. The two main peaks in toluene were correlated with benzene, and the toluene/benzene ratio was high, indicating that the air had not been processed extensively. The increases in gas-phase species, however, were not accompanied by parallel peaks in sub- μm POM, which strongly suggests that primary anthropogenic emissions of sub- μm POM were relatively insignificant. This observation was repeated several times during the cruise, and this explains why the primary

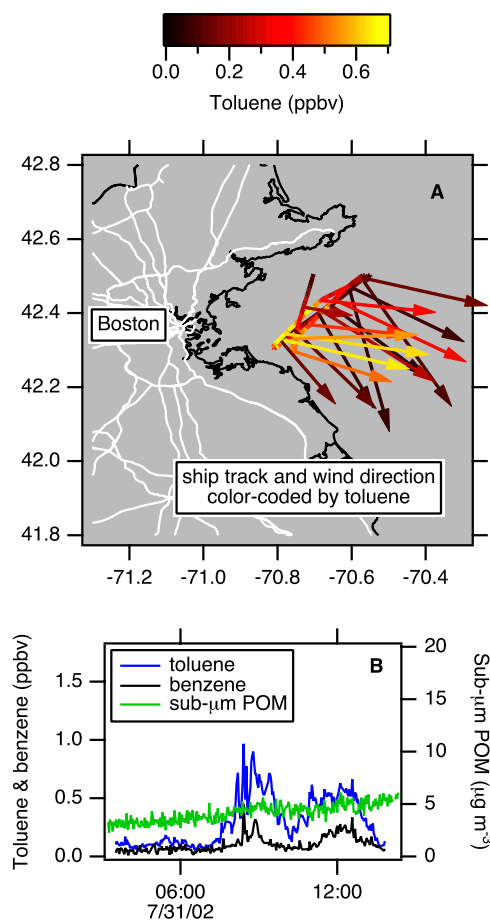


Figure 12. Example of sub- μm POM measurements in a nonprocessed urban plume. (a) Track of the *Ronald H. Brown* on July 31, 2002, color-coded by the measured mixing ratio of toluene. (b) Some of the measurement results during this period.

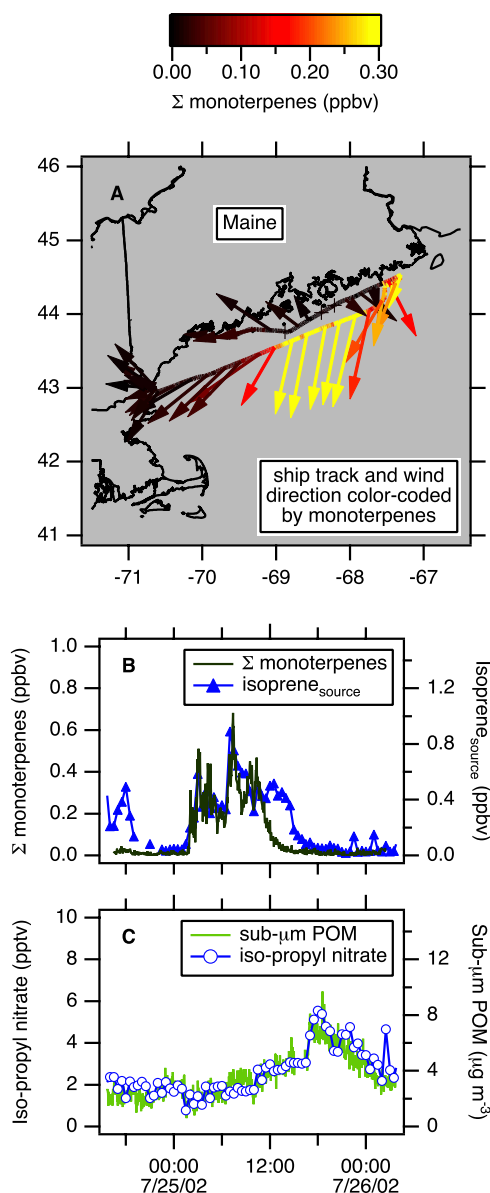


Figure 13. Example of sub- μm POM measurements in an air mass impacted by high monoterpene emissions in Maine. (a) Track of the *Ronald H. Brown* on July 25, 2002, color-coded by the measured mixing ratio of monoterpenes. (b and c) Some of the measurement results during this period.

anthropogenic fraction of sub- μm POM was determined to be small using the fit shown in Figure 11a.

[52] Figure 13 shows measurement results from a transect that the *Ronald H. Brown* made along the coast of Maine. Monoterpene emissions are particularly high in Maine [Geron *et al.*, 2000], and the ship indeed sampled air masses with total monoterpene mixing ratios of up to 600 pptv (Figures 13a and 13b). Figure 13c shows that the monoterpene peaks were not accompanied by parallel increases in sub- μm POM concentrations. In fact, Figure 13c shows that the sub- μm POM correlated well with the mixing ratio of iso-propyl nitrate during this period, strongly suggesting that the sub- μm POM was formed by secondary anthropo-

genic processes. Also shown in Figure 13b is the parameter isoprene_{source}, which is reasonably well correlated with the monoterpenes over this period, except at 12 pm UTC on July 24 and 25 (8 am local time). At these times, the OH levels in the atmosphere had built up to such levels that the monoterpenes emitted on land no longer reached the ship. Even in these air masses no influence of secondary POM formation from monoterpenes could be distinguished. This type of observation was made on several instances, which explains why the biogenic source of sub- μm POM was suggested to be small by the fit.

3.6. Budget of Organic Carbon

[53] The results from the fits shown in Figures 1–3, 6, 8, 9, and 11 allow an average description of organic carbon in a polluted air mass as a function of time (Figure 14). Figure 14a shows the calculation for alcohols, aldehydes, ketones and acids, using an equation that is slightly modified from equation (5):

$$[\text{OVOC}] = ER_{\text{OVOC}} \times \exp(-k_{\text{OVOC}}[\text{OH}]\Delta t) + ER_{\text{precursor}} \times \frac{k_{\text{precursor}}}{k_{\text{OVOC}} - k_{\text{precursor}}} \times (\exp(-k_{\text{precursor}}[\text{OH}]\Delta t) - \exp(-k_{\text{OVOC}}[\text{OH}]\Delta t)). \quad (7)$$

The first term in equation (7) represents the primary anthropogenic OVOC emissions, and the second term the formation and removal of secondary anthropogenic OVOCs. The biogenic and background term in equation (5) have been omitted, as we are interested here in the budget of anthropogenic organic carbon in the atmosphere. The parameters ER_{OVOC} , $ER_{\text{precursor}}$ and $k_{\text{precursor}}$ were taken from Table 1. Equation (7) describes the anthropogenic OVOC concentrations as a function of time for an urban air mass that has an acetylene mixing ratio of 1 ppbv at the time of emission. The OVOC concentrations in Figure 14a are given in units of $\mu\text{g C m}^{-3}$ to facilitate the comparison with organic carbon in the particulate phase. The carbon mass is used rather than the molecular mass: the mass of carbon does not change due to chemical conversion and should be a conserved quantity apart from deposition, or oxidation to species that were not measured during NEAQS.

[54] Figure 14a shows markedly different behaviors for the different classes of OVOCs. The ketones (acetone and MEK) have significant primary emissions and slowly increase as a result of secondary formation. The acids (formic and acetic acid) have no primary emissions and are exclusively secondary. The alcohols (methanol and ethanol) have no secondary sources and slowly decrease as time progresses. Finally, the aldehydes (acetaldehyde and propanal) are relatively independent of the photochemical age: their primary emissions are rapidly removed, but there is an efficient mechanism to regenerate aldehydes from a pool of precursors. Similar observations were made above in the discussion of Figure 8.

[55] Figure 14b shows the calculated evolution for the sub- μm POM. The concentration has been converted to organic carbon mass using the POM/POC ratio of 1.78 determined during NEAQS. Although the POM/POC ratio is expected to increase with age of the air mass (from

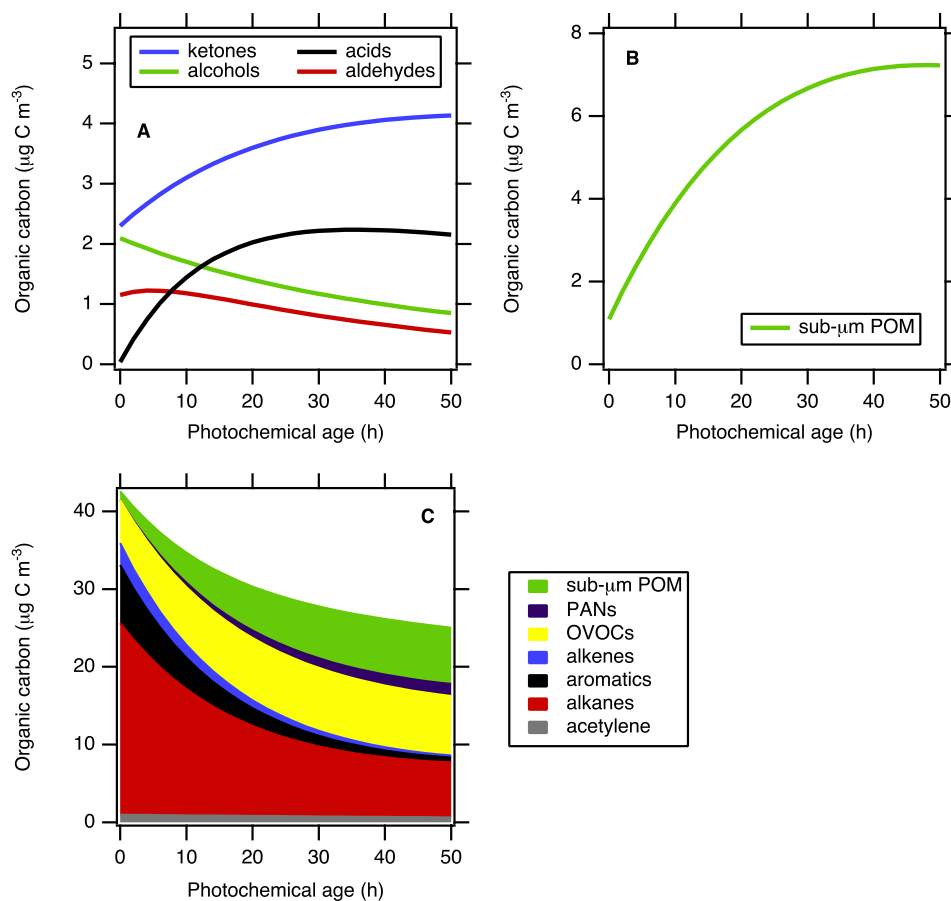


Figure 14. Budget of organic carbon from anthropogenic sources. (a and b) Temporal evolution of OVOCs and sub- μm POM, respectively, as determined in this work. The ketones include acetone and MEK, the alcohols include methanol and ethanol, the acids include formic and acetic acid, and the aldehydes include acetaldehyde and propanal. (c) Temporal evolution and speciation of the total organic carbon.

1.4 to 1.8 [Turpin and Lim, 2001]), there was no clear trend in the NEAQS data. Since the higher value of POM/POC is applied over the entire dataset, the effect of reducing it for the youngest air masses is to increase the amount of organic carbon emitted initially from 1 to 1.3 $\mu\text{g C m}^{-3}$ (see Figure 14b). The resulting increase in POM over the two-day period is 5.8 $\mu\text{g C m}^{-3}$ instead of 6.1 $\mu\text{g C m}^{-3}$. Thus, applying a constant POM/POC ratio of 1.78 does not have a significant effect on the carbon budget described here. The uncertainty in the POM/POC ratio itself, due to possible systematic errors in either the POM or POC measurement, is estimated to be about 25%. As a result, the uncertainty in the 2-day POM increase of 6.1 $\mu\text{g C m}^{-3}$ is thus also estimated to be 25%, i.e. 1.5 $\mu\text{g C m}^{-3}$. It is seen from Figure 14b that the primary emissions are a significant fraction of the total mass in the first few hours. The secondary formation continues for about two days, after which the total mass is almost exclusively from secondary sources.

[56] Figure 14c shows the time evolution of all organic carbon species attributed to anthropogenic sources. Also added to Figure 14c is the mass of peroxyacyl nitrates measured during NEAQS. As expected for secondary species, their mass is zero at the time of emission and

increases with time, but it remains a small fraction of the total mass. Not included in Figure 14c are the alkyl nitrate compounds. Their combined mass increases with the photochemical age (Figure 4b), but is small in comparison with the other species in Figure 14c. Figure 14c shows that shortly after emission most of the organic carbon is in the gas phase, mostly alkanes, whereas after two days, much of the mass has been converted to oxygenates and sub- μm POM. The remaining alkane fraction after two days is mostly ethane and propane. Several observations are made regarding Figure 14c and are discussed in the remainder of this section.

[57] The total mass of organic carbon decreases by about 40%. This may be due to deposition or to formation of species that are not accounted for in this study, such as difunctional species, CO, CO₂ and formaldehyde. Also, given the scatter in the data points (for example in Figure 4b) there is certainly a significant uncertainty in the temporal trend. Nevertheless, the analysis suggests that at least 60% of the total organic carbon, and most likely more, is accounted for in the analysis.

[58] Super- μm POC was quantified from filter samples, but was not included in this analysis, mostly because the measurement frequency was too low for a meaningful

description by equation (5). The super- μm POC was weakly correlated with the sub- μm POC ($r = 0.40$) and accounted on average for less than 20% of the sub- μm POC mass. Turekian *et al.* [2003] have shown that the super- μm POC associated with sea-salt aerosol, even though it contains only a small fraction of total POC, may account for a significant fraction of the dry deposition flux. This may contribute to the 40% decrease in total organic carbon observed in Figure 14c.

[59] Other gas-phase species that were not included in Figure 14c are CO, CO₂, methane and formaldehyde. In case of CO and CO₂ the secondary formation from VOCs is small in comparison with the ambient levels, and cannot be observed in an analysis like this. Methane is only slowly removed from the atmosphere and its contribution would essentially be constant over a period of 2 days. Formaldehyde was not measured during NEAQS and would probably represent a small but nonzero fraction of the organic carbon.

[60] Of all the primary hydrocarbons shown in Figure 14c, only the aromatics are assumed to be efficient precursors for secondary POM formation [Odum *et al.*, 1997]. However, it is interesting to note that the decrease of carbon mass associated with the aromatics is less than the increase of carbon mass due to secondary POM. Using the yields for the formation of secondary POM [Seinfeld and Pandis, 1998], we can estimate the total yield for the mixture of precursors that was determined for zero photochemical age (Figure 2):

$$\begin{aligned} \text{Total yield} = & \sum_{i=1}^{32} \text{Yield}_{\text{alkanes},i} \times ER_{\text{alkanes},i} \\ & + \sum_{j=1}^{10} \text{Yield}_{\text{alkenes},j} \times ER_{\text{alkenes},j} \\ & + \sum_{k=1}^{13} \text{Yield}_{\text{aromatics},k} \times ER_{\text{aromatics},k} \end{aligned} \quad (8)$$

Using this equation we find a total yield of $0.09 \mu\text{g C m}^{-3}$ for the alkanes, zero for the alkenes and $0.34 \mu\text{g C m}^{-3}$ for the aromatics, adding up to $0.43 \mu\text{g C m}^{-3}$. This number is clearly lower than the increase in POM in Figure 14b ($6.1 \mu\text{g C m}^{-3}$). The reasons for the discrepancy are not known, but may be that (1) the most important precursor VOCs were not measured during NEAQS, and/or (2) the formation of secondary POM is more efficient than determined in laboratory experiments.

[61] The question arises what fraction of the primary anthropogenic VOC emissions was not measured during NEAQS. Chung *et al.* [2003] have recently shown that in urban air masses that were recently impacted by emissions, only 5–15% of the total measured gas-phase organic carbon could not be identified using gas chromatography. Part of the unidentified fraction of the gas-phase organic carbon may consist of difunctional species such as glycolaldehyde, hydroxy acetone and (methyl) glyoxal as described by Spaulding *et al.* [2003]. Schauer *et al.* [1999, 2002a] have reported highly detailed emissions data for C₁–C₃₂ compounds in vehicle exhaust. The range of species measured during NEAQS (Figure 2) covers 82% of the total gas-phase emissions reported for gasoline vehicles [Schauer *et al.*,

2002a] and 55% of the total for medium duty diesel trucks [Schauer *et al.*, 1999]. As the fraction of diesel vehicles is only small (4%) [Kirchstetter *et al.*, 1999], we expect the fraction of the gas-phase organic carbon emissions identified during NEAQS to be close to 80% on average. In our analysis, 5–20% of the gas-phase organic carbon at zero photochemical age represents $2\text{--}7 \mu\text{g C m}^{-3}$. For gasoline vehicles the VOCs not measured during NEAQS included branched alkanes, branched alkenes and aldehydes, none of which are known to have particularly high POM formation yields [Seinfeld and Pandis, 1998]. The same holds for diesel trucks, in which a large fraction of the nonobserved emissions consists of aldehydes. In addition, the highest yields for forming secondary POM reported by Seinfeld and Pandis [1998] (for C₁₅-cycloparaffins) indicate that only 18% of the VOC mass goes into the particle phase. For these reasons it seems unlikely that all of the secondary POM formation observed in Figure 14b can be attributed to nonobserved precursors.

[62] There are several indications in the recent literature that secondary formation of POM may be more efficient than observed in the smog chamber experiments summarized by Seinfeld and Pandis [1998]. Jang *et al.* [2002] reported significant production of POC via catalytic oxidation of carbonyls on surfaces of acidic aerosols. A number of recent papers have reported secondary POM formation from species like isoprene that traditionally have not been regarded as precursors for aerosol formation [Limbeck *et al.*, 2003; Claeys *et al.*, 2004]. This suggests that POM formation may also be possible for other short-chain alkenes and perhaps alkanes. Additionally, Kalberer *et al.* [2004] identified polymers as an important component of aerosol from aromatic precursors. Interestingly, these authors hypothesized that glyoxal, methyl glyoxal and other, highly oxygenated species were important intermediates in this polymerization. We note here that glyoxals are not exclusive products to aromatic hydrocarbons but can also be formed from precursors such as isoprene and propylene (from the Master Chemical Mechanism v2.0 described by Jenkin *et al.* [1997]). The work of Limbeck *et al.* [2003], Claeys *et al.* [2004], and Kalberer *et al.* [2004] thus suggests that a much larger fraction of the gas-phase precursors observed in this work can contribute to the formation of secondary POM, which might account for the increase in sub- μm POM mass observed in Figure 14c.

[63] The largest uncertainty in the analysis presented in this paper may be the role of biogenic hydrocarbons. The atmosphere off the northeastern U.S. coast was strongly influenced by isoprene and monoterpene emissions [Warneke *et al.*, 2004; Goldan *et al.*, 2004], and it is difficult to rule out that some of these compounds contributed to the formation of OVOCs and sub- μm POM in Figure 14c. Our findings that (1) the sub- μm POM correlated well with iso-propyl nitrate, a secondary anthropogenic compound with no biogenic sources (Figure 10b), (2) the PAN compounds were, for the most part, correctly attributed to their respective biogenic and anthropogenic sources (section 3.4; Table 2), and (3) the biogenic contributions of OVOCs agreed with literature values (section 3.3; Table 4) certainly improve our confidence in the method. Other checks that we have performed include the use of biogenic indicators other than isoprene_{source} to

determine the biogenic fraction of the sub- μm POM (MPAN, monoterpenes, etc.). In all of these cases, however, the inferred biogenic contribution was small relative to the secondary anthropogenic source. Nevertheless, a complete separation of biogenic and anthropogenic precursors to the secondary POM formation is a complicated problem and cannot be fully addressed using the NEAQS data set.

[64] The relatively small biogenic fraction of POM inferred from the NEAQS data seemingly contradicts the radiocarbon measurements of POM that suggest a much higher fraction [Klinedinst and Currie, 1999]. A possible explanation for the discrepancy may be that the incorporation of biogenic species into the POM is much more efficient in polluted air. It was suggested above that a nonzero fraction of MPAN was attributed to secondary anthropogenic sources because NO_x plays a role in its formation, and the same might be true for POM. If NO_x or another pollution factor enhances the formation of POM from biogenic precursors, then the method developed here may attribute the POM to secondary anthropogenic sources, even though the organic carbon is of biogenic origin. It could also explain why the formation of POM was difficult to explain from anthropogenic precursors only. Nevertheless, these arguments are purely speculative at this point and much more work is necessary to study these processes.

4. Conclusion and Future Work

[65] An extensive set of organic carbon species in the gas and particle phase was measured in polluted and clean air masses off the northeastern U.S. coast during the New England Air Quality Study in 2002. The measurement results were used to study the budget of organic carbon, and an attempt was made to separate the sources of organic carbon quantitatively using gas-phase indicators for primary anthropogenic emissions, the photochemical age and biogenic sources. The approach was verified by comparing (1) the apparent rates at which hydrocarbons were removed from the atmosphere with the expected rates from OH oxidation, and (2) the hydrocarbon ratios extrapolated to zero photochemical age with the average composition of urban air. Additionally, the increase of the concentration of an alkyl nitrate with time could be explained in terms of a simple chemical kinetics description. In the case of OVOCs the results were compared with the limited amount of information that has been published, and a reasonable agreement was obtained. This work suggests that most of the organic carbon in the particle phase was formed via secondary anthropogenic processes. The results from the analysis are used to describe the combined mass of organic carbon in the gas and particle phase as a function of time. At the time of emission gas-phase species dominate the budget, but after two days OVOCs and POM form a significant fraction of the total organic carbon mass. It was difficult to explain the secondary formation of POM in terms of the removal of its traditionally recognized precursors.

[66] The present study only indicates what happens to organic carbon during the first two days after emission, and it will be of interest, although difficult, to follow the organic carbon composition of an air mass over a longer period. Additionally, the amount of data collected in close vicinity to emission sources was very limited during this experiment

-due to the nature of ship-based sampling of urban pollution- and it will be of interest to combine studies such as these with the results from similarly detailed measurements in an urban air shed. Finally, it will be of interest to perform a similar study in regions of the atmosphere that are more and less impacted by biogenic emissions, such that the conclusions about the separation of biogenic and anthropogenic sources can be verified.

[67] **Acknowledgments.** Helpful discussions with Michael Trainer, Chuck Brock, Dan Murphy, Greg Frost, and A. R. Ravishankara of the Aeronomy Laboratory, Jose Jimenez of the University of Colorado, Thomas Karl of NCAR, and Rainer Volkamer of MIT are gratefully acknowledged. We thank the crew and support team of the *Ronald H. Brown* and our NEAQS collaborators. Partial support for this work was provided by the National Science Foundation through awards to UVA (ATM-0207786) and UNH/MWO (ATM-0207646) and by NOAA Office of Oceanic and Atmospheric Research under grants NA17RP2632 and NA03OAR4600122 to UNH.

References

- Alfarra, M. R., et al. (2004), Characterization of urban and regional organic aerosols in the Lower Fraser Valley using two Aerodyne aerosol mass spectrometers, *Atmos. Environ.*, **38**, 5745–5758.
- Angevine, W. M., et al. (2004), Coastal boundary layer influence on pollutant transport in New England, *J. Appl. Meteorol.*, **43**, 1425–1437.
- Atkinson, R. (2000), Atmospheric chemistry of VOCs and NO_x , *Atmos. Environ.*, **34**, 2063–2101.
- Atkinson, R., and J. Arey (2003), Atmospheric degradation of volatile organic compounds, *Chem. Rev.*, **103**, 4605–4638.
- Baker, B., A. Guenther, J. Greenberg, and R. Fall (2001), Canopy level fluxes of 2-methyl-3-buten-3-ol, acetone and methanol by a portable relaxed eddy accumulation system, *Environ. Sci. Technol.*, **35**, 1701–1708.
- Bates, T. S., D. J. Coffman, D. S. Covert, and P. K. Quinn (2002), Regional marine boundary layer aerosol size distributions in the Indian, Atlantic, and Pacific Oceans: A comparison of INDOEX measurements with ACE-1, ACE-2, and Aerosols99, *J. Geophys. Res.*, **107**(D19), 8026, doi:10.1029/2001JD001174.
- Bertman, S. B., et al. (1995), Evolution of alkyl nitrates with air mass age, *J. Geophys. Res.*, **100**, 22,805–22,813.
- Biesenthal, T. A., and P. B. Shepson (1997), Observations of anthropogenic inputs of the isoprene oxidation products methyl vinyl ketone and methacrolein to the atmosphere, *Geophys. Res. Lett.*, **24**, 1375–1378.
- Bonsang, B., M. Kanakidou, G. Lambert, and P. Monfray (1988), The marine source of $\text{C}_2\text{-C}_6$ aliphatic hydrocarbons, *J. Atmos. Chem.*, **6**, 3–20.
- Borbon, A., H. Fontaine, M. Veillerot, N. Locoge, J. C. Galloo, and R. Guillermo (2001), An investigation into the traffic-related fraction of isoprene at an urban location, *Atmos. Environ.*, **35**, 3749–3760.
- Carter, W. P. L. (1990), A detailed mechanism for the gas-phase atmospheric reactions of organic compounds, *Atmos. Environ., Part A*, **24**, 481–518.
- Chung, M. Y., C. Maris, U. Krischke, R. Meller, and S. E. Paulson (2003), An investigation of the relationship between total non-methane organic carbon and the sum of speciated hydrocarbons and carbonyls measured by standard GC/FID: measurements in the Los Angeles air basin, *Atmos. Environ.*, **37**, suppl. 2, S159–S170.
- Claeys, M., et al. (2004), Formation of secondary organic aerosols through photooxidation of isoprene, *Science*, **303**, 1173–1176.
- DeBell, L. J., R. W. Talbot, J. E. Dibb, J. W. Munger, E. V. Fischer, and S. E. Frolking (2004), A major regional air pollution event in the northeastern United States caused by extensive forest fires in Quebec, Canada, *J. Geophys. Res.*, **109**(D19), D19305, doi:10.1029/2004JD004840.
- de Gouw, J. A., et al. (2003a), Validation of proton transfer reaction-mass spectrometry (PTR-MS) measurements of gas-phase organic compounds in the atmosphere during the New England Air Quality Study (NEAQS) in 2002, *J. Geophys. Res.*, **108**(D21), 4682, doi:10.1029/2003JD003863.
- de Gouw, J. A., C. Warneke, D. D. Parrish, J. S. Holloway, M. Trainer, and F. C. Fehsenfeld (2003b), Emission sources and ocean uptake of acetonitrile (CH_3CN) in the atmosphere, *J. Geophys. Res.*, **108**(D11), 4329, doi:10.1029/2002JD002897.
- Ehhalt, D. H., F. Rohrer, A. Wahner, M. J. Prather, and D. R. Blake (1998), On the use of hydrocarbons for the determination of tropospheric OH concentrations, *J. Geophys. Res.*, **103**, 18,981–18,997.

- Fall, R. (1999), Biogenic emissions of volatile organic compounds from higher plants, in *Reactive Hydrocarbons in the Atmosphere*, edited by C. N. Hewitt, pp. 41–96. Elsevier, New York.
- Faust, B. C., C. Anastasio, J. M. Allen, and T. Arakaki (1993), Aqueous-phase photochemical formation of peroxides in authentic cloud and fog waters, *Science*, *260*, 73–75.
- Fortin, T. J., B. J. Howard, D. D. Parrish, P. D. Goldan, W. C. Kuster, E. L. Atlas, and R. A. Harley (2005), Trends in U.S. benzene emissions inferred from atmospheric measurements, *Environ. Sci. Technol.*, *39*, 1403–1408.
- Fukui, Y., and P. V. Doskey (1998), Air-surface exchange of nonmethane organic compounds at a grassland site: Seasonal variations and stressed emission, *J. Geophys. Res.*, *103*, 13,153–13,168.
- Galbally, I. E., and W. Kirstine (2002), The production of methanol by flowering plants and the global cycle of methanol, *J. Atmos. Chem.*, *43*, 195–229.
- Geron, C., R. Rasmussen, R. R. Arnts, and A. Guenther (2000), A review and synthesis of monoterpene speciation from forests in the United States, *Atmos. Environ.*, *34*, 1761–1781.
- Glasius, M., et al. (2001), Relative contribution of biogenic and anthropogenic sources to formic and acetic acids in the atmospheric boundary layer, *J. Geophys. Res.*, *106*, 7415–7426.
- Goldan, P. D., W. C. Kuster, E. Williams, P. C. Murphy, F. C. Fehsenfeld, and J. Meagher (2004), Nonmethane hydrocarbon and oxy hydrocarbon measurements during the 2002 New England Air Quality Study, *J. Geophys. Res.*, *109*(D21), D21309, doi:10.1029/2003JD004455.
- Grosjean, D. E. Grosjean, and A. W. Gertler (2001), On-road emission of carbonyls from light-duty and heavy-duty vehicles, *Environ. Sci. Technol.*, *35*, 45–53.
- Guenther, A., et al. (1995), A global model of natural volatile organic compound emissions, *J. Geophys. Res.*, *100*, 8873–8892.
- Harley, R. A., and G. R. Cass (1994), Modeling the concentrations of gas-phase toxic organic air pollutants: direct emissions and atmospheric formation, *Environ. Sci. Technol.*, *28*, 88–98.
- Harley, R. A., M. P. Hannigan, and G. R. Cass (1992), Respeciation of organic gas emissions and the detection of excess unburned gasoline in the atmosphere, *Environ. Sci. Technol.*, *26*, 2395–2408.
- Heikes, B. G., et al. (2002), Atmospheric methanol budget and ocean implication, *Global Biogeochem. Cycles*, *16*(4), 1133, doi:10.1029/2002GB001895.
- Jacob, D. J., B. D. Field, E. M. Jin, I. Bey, Q. Li, J. A. Logan, R. M. Yantosca, and H. B. Singh (2002), Atmospheric budget of acetone, *J. Geophys. Res.*, *107*(D10), 4100, doi:10.1029/2001JD000694.
- Jang, M., N. M. Czoschke, S. Lee, and R. M. Kamens (2002), Heterogeneous atmospheric aerosol production by acid-catalyzed particle-phase reactions, *Science*, *298*, 814–817.
- Jayne, J. T., D. C. Leard, X. Zhang, P. Davidovits, K. A. Smith, C. E. Kolb, and D. R. Worsnop (2000), Development of an aerosol mass spectrometer for size and composition analysis of submicron particles, *Aerosol Sci. Technol.*, *33*, 49–70.
- Jenkin, M. E., S. M. Saunders, and M. J. Pilling (1997), The tropospheric degradation of volatile organic compounds: a protocol for mechanism development, *Atmos. Environ.*, *31*, 81–204.
- Jimenez, J. L., et al. (2003), Ambient aerosol sampling using the Aerodyne aerosol mass spectrometer, *J. Geophys. Res.*, *108*(D7), 8425, doi:10.1029/2001JD001213.
- Kalberer, M., et al. (2004), Identification of polymers as major components of atmospheric organic aerosols, *Science*, *303*, 1659–1662.
- Karl, T., A. Guenther, C. Spirig, A. Hansel, and R. Fall (2003), Seasonal variation of biogenic VOC emissions above a mixed hardwood forest in northern Michigan, *Geophys. Res. Lett.*, *30*(23), 2186, doi:10.1029/2003GL018432.
- Keene, W. C., and J. N. Galloway (1988), The biogeochemical cycling of formic and acetic acids through the troposphere: An overview of current understanding, *Tellus, Ser. B*, *40*, 322–334.
- Keene, W. C., et al. (1989), An intercomparison of measurement systems for vapor- and particulate-phase concentrations of formic and acetic acids, *J. Geophys. Res.*, *94*, 6457–6471.
- Keene, W. C., A. A. P. Pszenny, J. R. Maben, E. Stevenson, and A. Wall (2004), Closure evaluation of size-resolved aerosol pH in the New England coastal atmosphere during summer, *J. Geophys. Res.*, *109*(D23), D23307, doi:10.1029/2004JD004801.
- Kesselmeier, J., et al. (1997), Emission of short chained organic acids, aldehydes and monoterpenes from *Quercus ilex* L. and *Pinus pinea* L. in relation to physiological activities, carbon budget and emission algorithms, *Atmos. Environ.*, *31*, 119–133.
- Kesselmeier, J., K. Bode, C. Gerlach, and E.-M. Jork (1998), Exchange of atmospheric formic and acetic acids with trees and crop plants under controlled chamber and purified air conditions, *Atmos. Environ.*, *32*, 1765–1775.
- Kirchstetter, T. W., R. A. Harley, N. M. Kreisberg, M. R. Stolzenburg, and S. V. Hering (1999), On-road measurements of fine particle and nitrogen oxide emissions from light- and heavy-duty motor vehicles, *Atmos. Environ.*, *33*, 2955–2968.
- Kirstine, W., I. Galbally, Y. Ye, and M. Hooper (1998), Emissions of volatile organic compounds (primarily oxygenated species) from pasture, *J. Geophys. Res.*, *103*, 10,605–10,619.
- Klinedinst, D. B., and L. A. Currie (1999), Direct quantification of PM_{2.5} fossil and biomass carbon within the Northern Front Range Air Quality Study's domain, *Environ. Sci. Technol.*, *33*, 4146–4154.
- Kristensson, A., et al. (2004), Real-world traffic emission factors of gases and particles measured in a road tunnel in Stockholm, Sweden, *Atmos. Environ.*, *38*, 657–673.
- Li, S.-M., K. G. Anlauf, H. A. Wiebe, J. W. Bottenheim, P. B. Shepson, and T. Biesenthal (1997), Emission ratios and photochemical production efficiencies of nitrogen oxides, ketones, and aldehydes in the Lower Fraser Valley during the summer Pacific 1993 Oxidant Study, *Atmos. Environ.*, *31*, 2037–2048.
- Limbeck, A., M. Kulmala, and H. Puxbaum (2003), Secondary organic aerosol formation in the atmosphere via heterogeneous reaction of gaseous isoprene on acidic particles, *Geophys. Res. Lett.*, *30*(19), 1996, doi:10.1029/2003GL017738.
- MacDonald, R. C., and R. Fall (1993), Detection of substantial emissions of methanol from plants to the atmosphere, *Atmos. Environ., Part A*, *27*, 1709–1713.
- McKeen, S. A., and S. C. Liu (1993), Hydrocarbon ratios and photochemical history of air masses, *Geophys. Res. Lett.*, *20*, 2363–2366.
- McKeen, S. A., S. C. Liu, E. Y. Hsieh, X. Lin, J. D. Bradshaw, S. Smyth, G. L. Gregory, and D. R. Blake (1996), Hydrocarbon ratios during PEM-WEST A: A model perspective, *J. Geophys. Res.*, *101*, 2087–2109.
- Odum, J. R., T. P. W. Jungkamp, R. J. Griffin, R. C. Flagan, and J. H. Seinfeld (1997), The atmospheric aerosol-forming potential of whole gasoline vapor, *Science*, *276*, 96–99.
- Quinn, P. K., and T. S. Bates (2003), North American, Asian and Indian haze: Similar regional impacts on climate?, *Geophys. Res. Lett.*, *30*(11), 1555, doi:10.1029/2003GL016934.
- Ravishankara, A. R. (1997), Heterogeneous and multiphase chemistry in the troposphere, *Science*, *276*, 1058–1065.
- Roberts, J. M. (1990), The atmospheric chemistry of organic nitrates, *Atmos. Environ., Part A*, *24*, 243–287.
- Roberts, J. M., F. C. Fehsenfeld, S. C. Liu, M. J. Bollinger, C. Hahn, D. L. Albritton, and R. E. Sievers (1984), Measurements of aromatic hydrocarbon ratios and NO_x concentrations in the rural troposphere: Estimates of air mass photochemical age and NO_x removal rate, *Atmos. Environ.*, *18*, 2421–2432.
- Roberts, J. M., et al. (2002), Ground-based measurements of peroxyacetic nitric anhydrides (PANs) during the 1999 Southern Oxidants Study Nashville Intensive, *J. Geophys. Res.*, *107*(D21), 4554, doi:10.1029/2001JD000947.
- Rogge, W. F., L. M. Hildemann, M. A. Mazurek, G. R. Cass, and B. R. T. Simoneit (1996), Mathematical modeling of atmospheric fine particle associated primary organic compound concentrations, *J. Geophys. Res.*, *101*, 19,379–19,394.
- Salisbury, G., et al. (2003), Ground-based PTR-MS measurements of reactive organic compounds during the MINOS campaign in Crete, July–August 2001, *Atmos. Chem. Phys.*, *3*, 925–940.
- Sander, R., et al. (2003), Inorganic bromine in the marine boundary layer: A critical review, *Atmos. Chem. Phys.*, *3*, 1301–1336.
- Sander, S. P., et al. (2002), Chemical kinetics and photochemical data for use in atmospheric studies, Evaluation number 14, *JPL Publ.*, 02-25.
- Schade, G. W., and A. H. Goldstein (2001), Fluxes of oxygenated volatile organic compounds from a ponderosa pine plantation, *J. Geophys. Res.*, *106*, 3111–3123.
- Schauer, J. J., W. F. Rogge, L. M. Hildemann, M. A. Mazurek, G. R. Cass, and B. R. T. Simoneit (1996), Source apportionment of airborne particulate matter using organic compounds as tracers, *Atmos. Environ.*, *30*, 3837–3855.
- Schauer, J. J., M. J. Kleeman, G. R. Cass, and B. R. T. Simoneit (1999), Measurements of emissions from air pollution sources. 2. C1 through C30 organic compounds from medium duty diesel trucks, *Environ. Sci. Technol.*, *33*, 1578–1587.
- Schauer, J. J., M. J. Kleeman, G. R. Cass, and B. R. T. Simoneit (2002a), Measurements of emissions from air pollution sources. 5. C1 through C32 organic compounds from gasoline-powered motor vehicles, *Environ. Sci. Technol.*, *36*, 1169–1180.
- Schauer, J. J., M. P. Fraser, G. R. Cass, and B. R. T. Simoneit (2002b), Source reconciliation of atmospheric gas-phase and particulate-phase pollutants during a severe photochemical smog episode, *Environ. Sci. Technol.*, *36*, 3806–3814.

- Schauer, J. J., et al. (2003), ACE-Asia intercomparison of a thermal-optical method for the determination of particle-phase organic and elemental carbon, *Environ. Sci. Technol.*, *37*, 993–1001.
- Seila, R. L., W. A. Lonneman, and S. A. Meeks (1989), Determination of C₂ to C₁₂ ambient air hydrocarbons in 39 U.S. cities, from 1984 through 1986, *Rep. EPA/600/S3-89/059*, U.S. Environ. Prot. Agency, Washington, D. C.
- Seinfeld, J. H., and S. N. Pandis (1998), *Atmospheric Chemistry and Physics*, John Wiley, Hoboken, N. J.
- Shi, J., and M. J. Bernhard (1997), Kinetic studies of Cl-atom reactions with selected aromatic compounds using the photochemical reactor-FTIR spectroscopy technique, *Int. J. Chem. Kinet.*, *29*, 349–358.
- Singh, H., Y. Chen, A. Staudt, D. Jacob, D. Blake, B. Heikes, and J. Snow (2001), Evidence from the Pacific troposphere for large global sources of oxygenated organic compounds, *Nature*, *410*, 1078–1081.
- Singh, H. B., et al. (2003), Oxygenated volatile organic chemicals in the oceans: Inferences and implications based on atmospheric observations and air-sea exchange models, *Geophys. Res. Lett.*, *30*(16), 1862, doi:10.1029/2003GL017933.
- Sive, B. C., Y. Zhou, R. Russo, and R. Talbot (2003), Propane and light alkene enhancements at Thompson Farm: Impact on local and regional ozone production, *Eos Trans. AGU*, *84*(46), Fall Meet. Suppl., Abstract A41A-07.
- Spaulding, R. S., G. W. Schade, A. H. Goldstein, and M. J. Charles (2003), Characterization of secondary atmospheric photooxidation products: Evidence for biogenic and anthropogenic sources, *J. Geophys. Res.*, *108*(D8), 4247, doi:10.1029/2002JD002478.
- Stroud, C. A., et al. (2001), Isoprene and its oxidation products, methacrolein and methylvinyl ketone, at an urban forested site during the 1999 Southern Oxidants Study, *J. Geophys. Res.*, *106*, 8035–8046.
- Turekian, V. C., S. A. Macko, and W. C. Keene (2003), Concentrations, isotopic compositions, and sources of size-resolved, particulate organic carbon and oxalate in near-surface marine air at Bermuda during spring, *J. Geophys. Res.*, *108*(D5), 4157, doi:10.1029/2002JD002053.
- Turpin, B. J., and H. Lim (2001), Species contribution to PM_{2.5} concentrations: Revisiting common assumptions for estimating organic mass, *Aerosol Sci. Technol.*, *35*, 602–610.
- Warneke, C., et al. (2004), Comparison of daytime and nighttime oxidation of biogenic and anthropogenic VOCs along the New England coast in summer during New England Air Quality Study 2002, *J. Geophys. Res.*, *109*(D10), D10309, doi:10.1029/2003JD004424.
- Williams, J., et al. (1997), Regional ozone from biogenic hydrocarbons deduced from airborne measurements of PAN, PPN, and MPAN, *Geophys. Res. Lett.*, *24*, 1099–1102.
- Williams, J., et al. (2000), A method for the airborne measurement of PAN, PPN and MPAN, *J. Geophys. Res.*, *105*, 28,943–28,960.
- Zhou, X., and K. Mopper (1997), Photochemical production of low-molecular-weight carbonyl compounds in seawater and surface microlayer and their air-sea exchange, *Mar. Chem.*, *56*, 201–213.
-
- T. S. Bates, Pacific Marine Environmental Laboratory, NOAA, Seattle, WA 98115, USA.
- S. B. Bertman and M. Marchewka, Department of Chemistry, Western Michigan University, Kalamazoo, MI 49008, USA.
- M. R. Canagaratna and D. R. Worsnop, Aerodyne Research Inc., Billerica, MA 01821-3976, USA.
- J. A. de Gouw, F. C. Fehsenfeld, P. D. Goldan, W. C. Kuster, A. M. Middlebrook, J. M. Roberts, and C. Warneke, Aeronomy Laboratory, NOAA, Boulder, CO 80303, USA. (jdegouw@al.noaa.gov)
- W. C. Keene, Department of Environmental Sciences, University of Virginia, Charlottesville, VA 22903, USA.
- A. A. P. Pszenny, Institute for the Study of Earth, Oceans, and Space, University of New Hampshire, Durham, NH 03824, USA.